Transportation Consortium of South-Central States

Solving Emerging Transportation Resiliency, Sustainability, and Economic Challenges through the Use of Innovative Materials and Construction Methods: From Research to Implementation

The Impact of Hurricane Harvey on Pavement Structures in the South East Texas and South West Louisiana

Project No. 18PUTA02

Lead University: University of Texas at Arlington

Final Report

October 2019

Disclaimer

The contents of this report reflect the views of the authors, who are responsible for the facts and the accuracy of the information presented herein. This document is disseminated in the interest of information exchange. The report is funded, partially or entirely, by a grant from the U.S. Department of Transportation's University Transportation Centers Program. However, the U.S. Government assumes no liability for the contents or use thereof.

Acknowledgements

The authors would like to acknowledge the financial support for this study by the Transportation Consortium of South-Central States (Tran-SET) and the support with sample PMS data provided by Steven Loo and Shiva Singh with the City of Houston.

TECHNICAL DOCUMENTATION PAGE

1. Project No.	2. Government Accession No.	3. Recipient's Catalog No.
18PUTA02		

4. Title and Subtitle	5. Report Date
The Impact of Hurricane Harvey on Pavement Structures in the South East Texas and South West Louisiana	Oct. 2019
	6. Performing Organization Code
7. Author(s)	**8. Performing Organization Report No.**
PI: Stefan Romanoschi https://orcid.org/0000-0002-3051-3320	
9. Performing Organization Name and Address	**10. Work Unit No. (TRAIS)**
Transportation Consortium of South-Central States (Tran-SET) University Transportation Center for Region 6 3319 Patrick F. Taylor Hall, Louisiana State University, Baton Rouge, LA 70803	**11. Contract or Grant No.** 69A3551747106
12. Sponsoring Agency Name and Address	**13. Type of Report and Period Covered**
United States of America Department of Transportation Research and Innovative Technology Administration	Final Research Report Mar. 2018 – Mar. 2019
	14. Sponsoring Agency Code

15. Supplementary Notes

Report uploaded and accessible at Tran-SET's website (http://transet.lsu.edu/)

16. Abstract

This study developed a methodology to estimate the damage caused by flooding, such that caused by Hurricane Harvey, on a road or street network. The flooded street or pavement sections are identified using GIS flood maps with street GIS maps used for pavement management systems (PMS) by cities or state authorities. Then the damage caused by flooding directly through the increase moisture in foundation layers or indirectly due to the increase heavy traffic during the relief effort is estimated. An example Excel macro was created to illustrate the estimation process. The methodology estimates the increase in rehabilitation costs since the flooding imposes that many rehabilitation works must be done earlier than anticipated before the flooding. The methodology also estimated the increase in fuel consumption caused by the increased in pavement roughness if the rehabilitation works are done when anticipated before the flooding.

The methodology and the Excel macro can also be used to identify the pavement structures with better resilience to the flooding by grouping sections based on the flooding duration (no flooding, single and multiple day flooding) and on design features such as pavement type, functional class, age or time from the most recent resurfacing or reconstruction, subgrade soil type, traffic volume, layer thickness. In the case of networks with large number of sections, grouping done based on multiple criteria can allow detailed comparison and identification of design feature with more impact on the resiliency to flooding. ANOVA and MANOVA technique can be used to compare the Z-score values calculated for the reduction in PCI due to flooding for sections in different groups.

The methodology compares for each street or pavements section the measured condition after the flooding with that predicted based on data collected in multiple condition surveys before the flooding. It considers each road or street section as having unique design features, in-service conditions and therefore, unique performance.

17. Key Words	18. Distribution Statement
Flooded pavements, Pavement condition, Fuel consumption	No restrictions. This document is available through the National Technical Information Service, Springfield, VA 22161.

19. Security Classif. (of this report)	20. Security Classif. (of this page)	21. No. of Pages	22. Price
Unclassified	Unclassified	44	

Form DOT F 1700.7 (8-72) **Reproduction of completed page authorized.**

SI* (MODERN METRIC) CONVERSION FACTORS

APPROXIMATE CONVERSIONS TO SI UNITS

Symbol	When You Know	Multiply By	To Find	Symbol
		LENGTH		
in	inches	25.4	millimeters	mm
ft	feet	0.305	meters	m
yd	yards	0.914	meters	m
mi	miles	1.61	kilometers	km
		AREA		
in^2	square inches	645.2	square millimeters	mm^2
ft^2	square feet	0.093	square meters	m^2
yd^2	square yard	0.836	square meters	m^2
ac	acres	0.405	hectares	ha
mi^2	square miles	2.59	square kilometers	km^2
		VOLUME		
fl oz	fluid ounces	29.57	milliliters	mL
gal	gallons	3.785	liters	L
ft^3	cubic feet	0.028	cubic meters	m^3
yd^3	cubic yards	0.765	cubic meters	m^3
		NOTE: volumes greater than 1000 L shall be shown in m^3		
		MASS		
oz	ounces	28.35	grams	g
lb	pounds	0.454	kilograms	kg
T	short tons (2000 lb)	0.907	megagrams (or "metric ton")	Mg (or "t")
		TEMPERATURE (exact degrees)		
^oF	Fahrenheit	5 (F-32)/9 or (F-32)/1.8	Celsius	^oC
		ILLUMINATION		
fc	foot-candles	10.76	lux	lx
fl	foot-Lamberts	3.426	$candela/m^2$	cd/m^2
		FORCE and PRESSURE or STRESS		
lbf	poundforce	4.45	newtons	N
lbf/in^2	poundforce per square inch	6.89	kilopascals	kPa

APPROXIMATE CONVERSIONS FROM SI UNITS

Symbol	When You Know	Multiply By	To Find	Symbol
		LENGTH		
mm	millimeters	0.039	inches	in
m	meters	3.28	feet	ft
m	meters	1.09	yards	yd
km	kilometers	0.621	miles	mi
		AREA		
mm^2	square millimeters	0.0016	square inches	in^2
m^2	square meters	10.764	square feet	ft^2
m^2	square meters	1.195	square yards	yd^2
ha	hectares	2.47	acres	ac
km^2	square kilometers	0.386	square miles	mi^2
		VOLUME		
mL	milliliters	0.034	fluid ounces	fl oz
L	liters	0.264	gallons	gal
m^3	cubic meters	35.314	cubic feet	ft^3
m^3	cubic meters	1.307	cubic yards	yd^3
		MASS		
g	grams	0.035	ounces	oz
kg	kilograms	2.202	pounds	lb
Mg (or "t")	megagrams (or "metric ton")	1.103	short tons (2000 lb)	T
		TEMPERATURE (exact degrees)		
^oC	Celsius	1.8C+32	Fahrenheit	^oF
		ILLUMINATION		
lx	lux	0.0929	foot-candles	fc
cd/m^2	$candela/m^2$	0.2919	foot-Lamberts	fl
		FORCE and PRESSURE or STRESS		
N	newtons	0.225	poundforce	lbf
kPa	kilopascals	0.145	poundforce per square inch	lbf/in^2

TABLE OF CONTENTS

LIST OF FIGURES

LIST OF TABLES

ACRONYMS, ABBREVIATIONS, AND SYMBOLS

CEER	Center for Earthwork Engineering Research
DCP	Dynamic Cone Penetrometer
DOT	Departments of Transportation
FDR	Full-Depth Reclaimed
FWD	Falling Weight Deflectometer
GPR	Ground Penetration Radar
IRI	International Roughness Index
LaDOTD	Louisiana Department of Transportation and Development
LTPP	Long-Term Pavement Performance
MEPDG	Mechanistic-Empirical Pavement Design Guide
NOAA	National Oceanographic and Atmospheric Association
NWC	National Water Center
NWM	National Water Model
PCI	Pavement Condition Index
PMS	Pavement Management System
RTS	Retained Tensile Strength
WTC	World Transport Convention

EXECUTIVE SUMMARY

In order to estimate the damage caused by flooding, such that caused by Hurricane Harvey, on a road or street network a new methodology has been developed. The methodology consists of two parts:

a. The identification of flooded street or pavement sections using GIS flood maps that can be overlapped with street GIS maps normally used for pavement management systems (PMS) by cities or state authorities.
b. The estimation of the increase in rehabilitation works due to the damage caused by flooding directly or indirectly. An example Excel macro was created to illustrate the estimation process. The methodology estimates the increase in rehabilitation costs due to the fact that many rehabilitation works must be done earlier than anticipated before the flooding. The methodology also estimated the increase in fuel consumption caused by the increased in pavement roughness if the rehabilitation works are done when anticipated before the flooding.

The methodology and the Excel macro can also be used to identify the pavement structures with better resilience to the flooding by grouping sections based on the flooding duration (no flooding, single and multiple day flooding) and on design features such as pavement type, functional class, age or time from the most recent resurfacing or reconstruction, subgrade soil type, traffic volume, layer thickness. In the case of networks with large number of sections, grouping done based on multiple criteria can allow detailed comparison and identification of design feature with more impact on the resiliency to flooding. ANOVA and MANOVA technique can be used to compare the Z-score values calculated for the reduction in pavement condition index (PCI) for sections in different groups.

The methodology compares for each street or pavements section the measured condition after the flooding with that predicted based on data collected in multiple condition surveys before the flooding. It considers each road or street section as having unique design features, in-service conditions and therefore, unique performance. Other methodologies assume that pavements having some similar design features should have the same performance. This approach is misleading since pavements with identical design features may perform differently due to difference in drainage quality, in geometrical features and in the quality of their construction or rehabilitation.

1. INTRODUCTION

The U.S. has been impacted with 250 weather and climatic disasters between 1980 and 2019, costing more than $1 billion per event. The total cost of these events exceeds $1.7 trillion, as estimated by the National Oceanic and Atmospheric Administration (NOAA) *(1)*. Twenty-two percent of these significant flooding events occurred in Texas *(2)*.

The most recent event that impacted Texas was Hurricane Harvey from August 28th through September 3rd, 2017. Hurricane Harvey is considered the worst natural disaster in the history of Texas. Harvey brought one of the most intense rainfall recorded in continental U.S. In a four-day period, many areas received more than 40 in of rain as the system meandered over eastern Texas and adjacent waters, causing catastrophic flooding. With peak accumulations of 51.88 in, Harvey is the wettest tropical cyclone on record in the contiguous U.S. The resulting floods inundated hundreds of thousands of homes, displaced more than 30,000 people, and prompted more than 17,000 rescues, bringing damage of $130 billion to the state of Texas *(1)*.

There are several studies providing predictions of amplification of flood frequencies that will impact coastal locations *(3, 4)*.The great concern after flooding events is the assessment of the damage caused by the sustained flooding on pavement structures. Therefore, it is necessary to have an in-depth understanding on the impact of such events on the pavement system.

This study will provide a methodology to evaluate the damage caused to pavement structures by flooding, such as the extensive flooding in the SE Texas and SW Louisiana during Hurricane Harvey. An agency managing a road or street network can use by comparing for each road or street section the pavement performance predicted from the condition survey data before the flooding with the condition data measured after the flooding. The methodology will provide a quantitative estimate of the costs for the rehabilitation of the road or street network that must be done earlier because of the flooding. The methodology also estimates the increase in fuel consumption and CO_2 emission if the rehabilitation actions are performed at the time planned before the flooding.

2. OBJECTIVES

The objective of this project is to develop a methodology for evaluating the effects of flooding on the performance of pavement structure. The methodology relies on the comparison of the condition of each road or street section measured after the flooding with the condition predicted from the surveys conducted before the flooding. The advantage of using a methodology that analysis each sections separately is that it does not compare the condition and performance of different section, which not only may have different design features (layer thicknesses and materials, soil subgrade) but also may carry different traffic volumes and weights before or after the flooding. In addition, road or street sections carrying the same traffic and having the same design features may have different efficiency of the drainage system. Moreover, the actual features and quality of work when they were built or rehabilitated may be different.

Since the methodology predicts for each section the measured condition after flooding to that predicted from the data collected in condition surveys before the flooding, it can estimate for each road or street sections how much sooner the rehabilitation works must be performed. This helps road or street managing agencies estimate the impact of flooding in terms of increased need for rehabilitation work. The agencies can also estimate the impact to the vehicle user costs if the rehabilitation works are done according to the original schedule instead of the new schedule, imposed by the damaging effect of the flooding.

3. LITERATURE REVIEW

3.1. Evaluation of the Effects of Flooding by Surveying In-Situ Pavement Sections

One of the very few efforts to investigate the damage caused by flooding to a road network is the study by Chen and Zhang *(5)*. They used PMS data collected by the Louisiana Department of Transportation and Development (LaDOTD) in District 02, covering the Greater New Orleans area. They compared the change in roughness and rutting between the last recorded values before Hurricanes Katrina and Rita (August and September 2005) and the corresponding values recorded first time after the hurricanes for each 0.1 mile road section. The PMS data showed and increased damage to the highways, as shown in Table 1.

The analysis of the data concluded that the average IRI values and IRI increments were higher for flexible and composite road sections in the flooded zone than for those in the non-flooded zone. The opposite was observed for concrete pavements, indicating that the concrete pavement structures were less affected by the hurricanes. A similar conclusion was drawn after analyzing the rutting data. However, it is important to note that the study does not discuss some important details such as the grouping of road sections within the same pavement type based on similar layer thickness, drainage system type or truck traffic volume. This grouping may provide additional information that can reinforce or weaken the conclusions drawn. Also, the paper does not discuss the length of time between the last condition survey before the hurricanes and the first condition survey after the hurricane. If it was not the same for all studied road sections; it might have an impact on the recorded jump in distress values and thus, on the validity of the conclusions drawn. The paper does not mention if the same automated system was used on all sections; the measuring equipment may have an impact on the recorded values also.

The merit of the study lies in the aim to study the entire road network in the New Orleans region, and it included road sections in flood and non-flood zones; many of these sections were possibly impacted also by the heavy trucks transporting debris and equipment used for the relief effort. This later impact cannot be quantified by modelling effects of saturated unbound layers for representative or typical pavement sections.

In 2007, Gaspard et al *(6)* conducted a study to assess the impact of Hurricane Katrina and Hurricane Rita on pavements in the New Orleans area. It was assumed that the pavements submerged in water are structurally damaged. The damages, in fact, were found in asphalt and concrete layers with weak subgrades. To evaluate the effects of flooding and estimate the cost of rehabilitation, PMS data collection was conducted by LaDOTD on 238 miles of state highways at 0.1 mile intervals. Using the GIS mapping of NOAA flood map on the street network, the data points where identified as submerged and non-submerged data. A two-way ANOVA was performed on the data set to test the hypothesis that the submerged pavements were damaged as a result of the hurricanes.

Table 1. Highly deteriorated pavements in District 02 based on IRI *(5)*.

Flood Zone	Pavement Type	Control Section Numbers	Total Length (Mile)	Highly Deteriorated Length (Mile)	Highly Deteriorated Length rate (%)	Ave IRI 2005 (in./mi.)	Ave IRI 2007 (in./mi.)	ΔIRI (in./mi.)
Flood Zone	Asphalt	19	91.2	5.8	6.3	134.2	181.8	47.7
Flood Zone	Composite	21	171.0	13.4	7.8	143.0	185.9	42.9
Flood Zone	Concrete	11	107.3	10.0	9.3	164.2	203.5	39.4
Flood Zone	Overall	51	369.4	29.2	7.9	147.1	190.4	43.3
Non-Flood Zone	Asphalt	62	294.0	34.5	11.7	127.8	169.9	42.1
Non-Flood Zone	Composite	46	301.1	30.6	10.2	120.0	153.1	33.1
Non-Flood Zone	Concrete	13	61.3	6.4	10.4	189.2	232.5	43.3
Non-Flood Zone	Overall	121	656.4	71.5	10.9	145.6	185.1	39.5
Overall	Overall	172	1025.8	100.6	9.8	146.4	187.8	41.4

The result of their study revealed that the strength loss of asphalt pavements was equivalent to about two inches of asphalt concrete. Also, it was observed that thinner pavement sections were more affected by flooding, so they require more structural repair in compare to the thicker pavement sections. For thick PCC pavements, very little relative damage was observed. However, analysis of the thinner PCC pavement showed that the structural loss because of the flooding is equivalent to 0.43 inches and 0.47 inches of asphalt, for the pavement layers and the subgrade, respectively. There was no need for additional pavement structure on composite pavement; however, subgrade strength loss caused a decrease in structural strength equivalent to 0.9 in. of asphalt concrete.

In another study to investigate the impact of Hurricane Katrina and Hurricane Rita on pavements, Helali et al. *(7)* analyzed the structural and functional performance of pavements in Jefferson Parish Louisiana. The PMS data set containing roughness, distress, deflection, and traffic data collected before and after the hurricanes were used to perform this analysis. Also, a statistical analysis was performed on the data set in order to examine the extent and significance of the damage. The results proved that there is a significant damage on the pavements which were submerged during the floods. The comparison between the flooded and non-flooded section of flexible pavements showed one unit drop in Structural Number, which is equivalent to 2.3 inches of asphalt concrete.

A study conducted by The Center for Earthwork Engineering Research (CEER) at Iowa State University on the effect of West Iowa Missouri River flood in 2011 estimated a damage of $63 million on primary and secondary roadways. The main objective of this study was to use advanced assessment technologies to evaluate rapidly the damage caused by flooding and develop a list of effective strategies for repair and mitigation of damages in future flooding events *(8)*.

The condition of pavements and surfaces including gravel roadways, chip seal over gravel bases, AC and PCC pavements were assessed using the Falling Weight Deflectometer (FWD), Dynamic Cone Penetrometer (DCP) and Ground Penetration Radar (GPR) tests, 3-D laser scanning, and

hand auger sampling. Due to lack of historical data before flooding, the assessment of damages caused by flooding was done by comparing the condition of flooded pavements with that of non-flooded pavements.

Their results indicated a significant difference in foundation supports in the flooded and non-flooded areas. These losses of supports were related to the voids in shallow depth (<6 in.) and deeper depth (>6 in.) due to erosion of base material and subgrade, respectively. Their statistical analysis on FWD test on gravel roads revealed that flood significantly affects the strength of the roads. The FWD measurement showed that that subgrade is 6 times more affected by the flood than the gravel layer is. In addition, a rut depth up to 4.9 inches deep was observed on gravel roadways.

FWD testing on asphalt pavements done six months after the flooding showed that the modulus of the asphalt and subgrade layers were 1.35 times higher in flooded area than in non-flooded areas. Also, no structural failure was observed on AC pavements. On the flooded PCC pavements longitudinal cracks were observed on some slabs due to loss of base course. Poor k_{static} values, ranging from 55 to 73 psi, were recorded. A catalog including field assessment techniques and potential repair and mitigation strategies was provided.

In a comprehensive study, Sultana et al. *(9–11)* investigated the effects of 2011 flooding in South-East Queensland, Australia, on the structural performance of pavements. These studies included FWD surface deflection data collection on flooded and non-flooded roads before and after flooding events. The data was used to back-calculate the elastic moduli of the pavement layers including the CBR of subgrade. The modified structural numbers from FWD maximum deflection was calculated using the following equation:

$$SNC = 3.2 \times D_0^{-0.63} \quad [1]$$

where:
SNC is modified structural number; and
D_0 is maximum deflection (mm) at load center.

To compare the flooded pavements to non-flooded ones, network level structural deterioration models for AC pavements and sealed unbound granular pavements were utilized, respectively, as following:

$$SNC_{ratio} = 0.991 \times (2 - e^{0.00132 \times TMI_i + 0.256 \times (\frac{AGE_i}{DL})}) \quad [2]$$

$$SNC_{ratio} = 0.9035 \times (2 - e^{0.0023 \times TMI_i + 0.1849 \times (\frac{AGE_i}{DL})}) \quad [3]$$

where:
SNC_{ratio} = current strength of pavement/subgrade relative to its initial strength (SNC_i/ SNC_0);
SNC_i = modified structural number at the age 'i' of measurement;
SNC_0 = modified structural number at the age 'i' of pavement construction;
TMI_i = Thornthwaite Moisture Index at the age 'i' of measurement;
AGE_i = age of pavement (since construction or last rehabilitation); and
DL = the design life of pavement.

After performing a statistical analysis, they observed a 25 to 40% increase in FWD surface deflection and up to 50% reduction in the structural strength of pavement sections. Also, it was observed that the subgrade CBR reduced by up to 67 percent. In case of partially flooded pavements, the flooded part of the section the pavement had lower structural strength compare to the non-flooded part. The rate of reduction in the Structural Number and CBR values for flooded pavements were observed to be faster than their normal deterioration rate. Moreover, this conclusion had been drawn that the impact of flooding may not be always visible immediately after the event, since it may only affect the structure of the pavement.

In their second study, they developed a deterministic model that expressed the structural strength of a flexible pavement as a function of time as shown in Equation 4 *(10)*. This model was capable of predicting the short-term behavior of the pavement immediately after the flooding (within 6 weeks).

$$SNC_{ratio\,f} = 1.032 - 0.034 \times e^{(\frac{t}{21.5})} \quad [4]$$

where:
$SNC_{ratio\,f}$ = ratio of modified structural number of the pavement after time t of flooding to modified structural number before flooding; and
t = the time in days (t<42 days).

Both the studies have some limitations. For developing their models, they used a sample of a road group with a similar traffic volume. In addition, no simulation was used to account for different probabilities of flooding. Their models estimate the performance of pavements within six weeks of flooding, but they over-predict the deterioration after six weeks. Therefore, the results may not assist in rehabilitation action selection.

In their most recent study *(11)*, they developed two mechanistic-empirical deterministic models for predicting the rutting and roughness of flooded pavements. The proposed models for rutting and roughness are given in Equations 5 and 6.

$$\Delta Rut_{post-flood} = k_{rut} \times [0.083 \times t^{0.85} + (0.109 \times Rut_{pre-flood}) - 0.746] \quad [5]$$

$$\Delta IRI_{post-flood} = k_{rg} \times [0.039 + 0.027 \times t^{0.5}] \quad [6]$$

where:
$\Delta Rut_{post-flood}$ = difference between post-flood rutting and pre-flood rutting (mm);
$Rut_{pre-flood}$ = pre-flood rutting (mm);
$\Delta IRI_{post-flood}$ = difference between post-flood IRI and pre-flood IRI (m/km);
t = time lapse in collection of rutting/IRI data after flood (t<172 days); and
k_{rut} and k_{rg} = local calibration factor for different types of pavement (default=1).

Since the original data set was collected within 25 weeks of flooding, the proposed models are valid in this timeframe and they might may not be applicable for longer periods. The authors claimed that the calibration of these models helps quantifying the loss of strength and surface condition of pavements immediate after flooding, but no longer-term effect are predicted.

3.2. Evaluation of the Effects of Flooding using Theoretical Models

Mallick et al. *(12)* developed a framework to simulate the long-term impact of climate change on pavement performance, and construction and maintenance costs. A dynamic system model was created using the available pavement performance and climate change data. To represent the climatic changes, four factors adversely affecting the pavement performance were considered: the increase in air temperature, increase in average annual rainfall, rise in seawater level and increase in number of hurricanes. The average pavement life and maintenance costs were predicted using the results of the modeling using the Mechanistic-Empirical Pavement Design Guide (MEPDG). In their analysis, they considered rutting as a primary distress and calculated the failure by rutting to estimate the pavement life.

The results indicated that the climate change significantly reduces the structural strength of subgrade soil and asphalt layers, and consequently the average pavement life decreases from 16 to 4 years. In their analysis of cost estimation, it was assumed the asphalt overlay as the only maintenance activity. It was estimated that the climate change increases the maintenance cost to more than 160 percent over the span of 100 years. The presented results dependent on specific pavement and the traffic used in their studies, but the study proved the drastic effect of climate change to pavement life.

In another study, Mallick et al. *(13)* presented a methodology and a software package to evaluate the contribution of pavement materials, climate and construction quality on the pavement's vulnerability to flood-induced damage. To develop this software, a dynamic system model was used to calculate the critical time ($T_{critical}$) for failure of the unbound base and the bound surface layer due to inundation. The pavement is predicted to be severely damaged during and immediately after flooding if the duration of flooding exceeds $T_{critical}$. They presented the following equation for computing $T_{critical}$:

$$t = \frac{\theta_s - \theta_i}{k}\left[L_f - (h_L - \psi_f)\ln\left(\frac{h_L + L_f - \psi_f}{h_L - \psi_f}\right)\right] \quad [7]$$

where:
θ = volumetric moisture content at saturation;
θ_i = initial volumetric moisture content;
L_f = thickness of HMA+base course in m;
ψ_f = suction in m;
h_L = depth pf ponded water in m;
t = time to infiltrate in seconds, and
k = permeability in m/s.

To account for the required time for water infiltration of HMA layer above the base course, an effective permeability was determined using the following equation:

$$k_{effective} = \frac{h_{HMA} + h_{base}}{\frac{h_{HMA}}{k_{HMA}} + \frac{h_{base}}{k_{base}}} \quad [8]$$

where:
$k_{effective}$ = effective permeability in m/s;

h_{HMA} = thickness of HMA in m;
h_{base} = the thickness of base course in m;
k_{HMA} and k_{base} = permeability of HMA and base course in m/s.

In their proposed model, they also considered the effect of erosion of the base course material on reduction in tensile strength of AC pavements when they are near a stream:

$$V_c = 0.35 * D_{50}^{0.45} \quad [9]$$

where:
V_c = critical flow velocity in m/s; and
D_{50} = particle size medium diameter in mm.

$$RTS(t) = RTS(i) - RRTS * t \quad [10]$$

$RTS(t)$ = retained tensile strength at any time t (%);
$RTS(i)$ = initial tensile strength;
$RRTS$ = rate of change in retained tensile strength (% per unit of time); and
t = time at which the retained tensile strength is determined (yr.).

The developed system dynamics model is shown in Figure 1.

The results derived from their framework revealed that the model was sensitive to the duration of inundation, aging resistance of asphalt binder, voids in the AC layer, existence of damages on AC and base course during the inundation, the thickness of AC and base courses as well as their permeability. This framework can be used as a risk analysis tool and to identify vulnerable pavements before flooding to either take action to improve them or to monitor them closely to find the flood-induced deterioration.

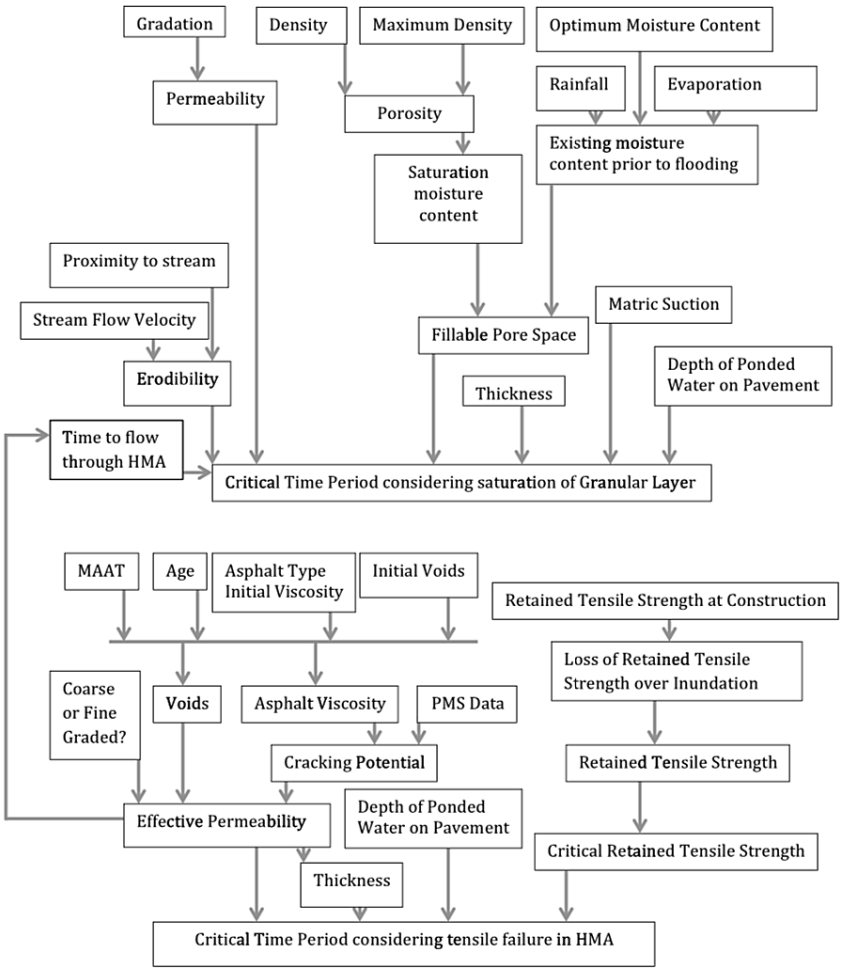

Figure 1. Model for determination of critical flooding time *(13)*.

Shamsabadi et al. *(14)* assessed the performance of highway pavements after snowstorms and flooding events. These impacts were quantified using data collected from long-term pavement performance (LTPP) and NOAA databases. Then considering the severity of the events and condition of the pavement prior to these events, through a regression based statistical method, models for snowstorms (Equation 11) and floods (Equation 1 – 12) were developed. The models have a coefficient of correlation, R^2, of more than 0.90.

$$\%\Delta IRI = 5.09 - 2.5NIRI + 1.7NDepth - 1.74NDuration + 0.706ESAL * Duration \quad [11]$$

$$\%\Delta IRI = 10.7 - 1.66NIRI + 7.30NDepth - 2.10NDuration + 14.3Depth * IRI \quad [12]$$

where:
$\%\Delta IRI$ = percent increase in IRI due to the snowstorm;
$NIRI$ = normalized IRI of the section before the snowstorm;
$NDepth$ = normalized depth of the snowfall;
$NDuration$ = normalized duration of the snowstorm; and
$ESAL$ = equivalent single-axle load.

Khan et al. *(15)* studied the performance of different pavement types against flooding to identify their resilience to flooding. They developed roughness and rutting-based deterioration models that employ the probability (Pr) of flooding, the duration of flooding, and loss of base course resilient modulus (MrL) and change in IRI due to flooding. For their analysis, they computed two gradients, $\Delta IRI/Pr$ and $\Delta IRI/MrL$ using the change in IRI versus the probability of flooding and the loss of resilient modulus MrL. Monte Carlo simulations were performed accounting for different probability of flooding, proposed gradients, and consequences of flooding.

The results proved that PCC and strong asphalt pavements are the most resilient to flooding. The authors claimed that the advantage of using the developed models contributes to assessing pavements in the flood prone areas before flooding, improving a Pavement Management System (PMS) with models incorporating flooding, and taking actions to minimize the risks. The outcomes help with choosing more effective maintenance strategies, having better pavement performances, and reducing service life maintenance costs. They suggested that pre-flood maintenance strategy is more effective than post-flood maintenance strategy. They recommended that and pavements strength in flood prone areas should be strengthened by adding overlays and/or layer stabilization.

In order to understand the performance of pavements during and after the flooding, Elshaer *(16)* performed a study aimed at identifying the most critical parameters affecting the performance of pavements. He also presented an alternative method to estimate FWD surface deflections and the bearing capacity of pavements in short term flooding, incorporate subgrade soil moisture into the analysis, and determine the flooded pavements' failure time. To evaluate the mechanical response of pavements during and after flooding, models used in MEPDG were utilized. The analysis was conducted using layered elastic methods. The effect of the parameters was examined using analysis of variance techniques.

The analysis showed that in-situ FWD deflection can be predicted using parameters such as moisture content, unbound material types, groundwater table, depth to bedrock, AC temperature and layer thickness. The analysis conducted on the effect of stress-dependency and moisture sensitivity of the unbound materials proved that using the available empirical models for the resilient modulus of unbound materials in layered elastic analysis were adequate to predict the in-situ deflection of to low plasticity soils. However, non-linear elastic analysis overestimated the FWD deflection of both cohesive and non-cohesive materials.

The findings showed that the base and subgrade material characterization are the most important parameters for rutting performance of pavements. In addition, it was found that the structural capacity of pavements reduces significantly when the pavement section is in fully saturated condition, but the value was regained after the water level drops. The water table level significantly affects the load distribution in the pavement layers, but its impact depends on pavement structure and material type. Also, the load carrying capacity of pavements were found to be greater in coarse soils in compare to the finer soils.

Asadi et al. *(17)* developed a framework to analyze the structural damage caused by moisture in flexible pavement structures. The framework integrated the unsaturated hydraulic analysis with finite element response modeling of flexible pavement. The former was used to estimate the evolution with time of the moisture content at various depth in the granular unbound materials.

The moisture content values were used to estimate the change of moduli of the unbound layer with time and depth. The strains calculated by the finite element program at critical locations were used to estimate the reduction in pavement life.

The framework was demonstrated for three flexible pavements with asphalt concrete surface over a full-depth reclaimed (FDR) base and granular subbase and with three drainage systems: side drain, subsurface drainage with drainage pipes clogged or not. The proposed framework can model various scenarios in terms of structural and drainage system configuration, and it can determine their resilience against extreme events that cause heavy precipitation. The pavement designer can thus evaluate the impact of drainage structures and conditions of pavement life and thus optimize the design solution.

The framework cannot study in-situ pavements since it is uses hypothetical scenarios. It does cannot model the infiltration through the sides of the pavement, the significant rise in water table due to flooding or infiltration of water below drainage layers or through the shoulders. It also cannot model a partially working drainage system. The use of computationally intensive models such as the finite element analysis limits the use of the framework to project level analysis; it cannot be used for the evaluation of resilience to extreme events of an existing road network analysis. However, it can be a very useful tool in selecting the best pavement structural configurations and drainage systems to resist heavy rainfall.

3.3. Summary

The effect of flooding on the pavement condition and performance has been the focus of several research studies. Most studies compared the bearing capacity pavement structures determined through Falling Weight Deflectometer (FWD) tests for flooded pavements to that of sections not flooded. FWD tests have been used to estimate the in-situ stiffness of pavement layers, which has been then used to estimate the number of standard axles to failure. This approach has the benefit of determining the bearing capacity and not recording and comparing distresses, which may not show in the first months after the flooding.

Using FWD test results right after the flooding may indicate a larger effect of flooding on layer moduli than if the FWD tests are conducted more than six weeks after the flooding. This suggests that the timing of the FWD testing may have an effect on the results of the comparison. The low stiffness of pavement layers does not remain low since the high moisture content in the unbound layers decreases with time; the bearing capacity computation might over- estimate the effect of the flood. Therefore, it is more reasonable to evaluate distresses after the flooding, even for a longer period to quantify the damaging effects of floods.

Other studies evaluated distresses after flooding and compared them with the distresses recorded before the flooding. The increase in distress levels is then compared for pavements in flooded areas to that of pavements in areas not flooded. This approach assumes that pavements with similar design features should have the same performance. This assumption is insufficient to ensure the validity of performance comparison. Pavements with the same design features may carry different traffic volumes and weight, may have different drainage systems with different drainage capabilities. The quality of the construction and rehabilitation on these pavements can be different also. All these differences may explain the intriguing finding reported by Chen and Zhang *(5)* for

the pavements on the Greater New Orleans area. In their comparison, flooded concrete pavements had a smaller increase in IRI after Hurricanes Katrina and Rita than non-flooded concrete pavements.

A few other studies proposed frameworks to estimate the damaging effect of flooding through theoretical modelling of pavement structures. Even though these frameworks may include advanced models for predicting moisture content changes in unbound layers and for computing the extent of distresses from the response of pavement structures under a reference wheel load, they cannot properly model several real life conditions such as the quality of the drainage system or existing distresses in in-situ pavements. In addition, they cannot model well the damage the exposure to water causes to pavement materials such a stripping of asphalt mixes, D-cracking, freeze-thaw cracking or Alkai-Silica Reaction (ASR).

4. METHODOLOGY

4.1. Flood Data Source

The determination of road and street sections flooded during a hurricane can be accomplished by obtaining flood maps provided by NOAA National Water Center (NWC) National Water Model (NWM). As an example, daily flood maps streamflow forecasts from NOAA and NWC were utilized to obtain the impact zone of Hurricane Harvey for the city of Houston *(18)*. Daily flood maps from August 28 to September 3, 2017, are available in the TIFF file format for 22 different basins including 120100, 120200, 120301, 120302, 120401, 120402, 120500, 120601, 120602, 120701, 120702, 120800, 120901, 120902, 120903, 120904, 121001, 121002, 121003, 121004, 121101, and 121102. To select the suitable basins for Houston city area, GIS referenced maps for the basins and street network were imported to the ArcGIS software package. After evaluating these basins in ArcGIS, basins 120401 and 120402 were found to be located in the city of Houston street map, as illustrated in Figure 2 where the Green color represents the Houston street network and the gray and the black colors represent 120401 and 120402 basins, respectively.

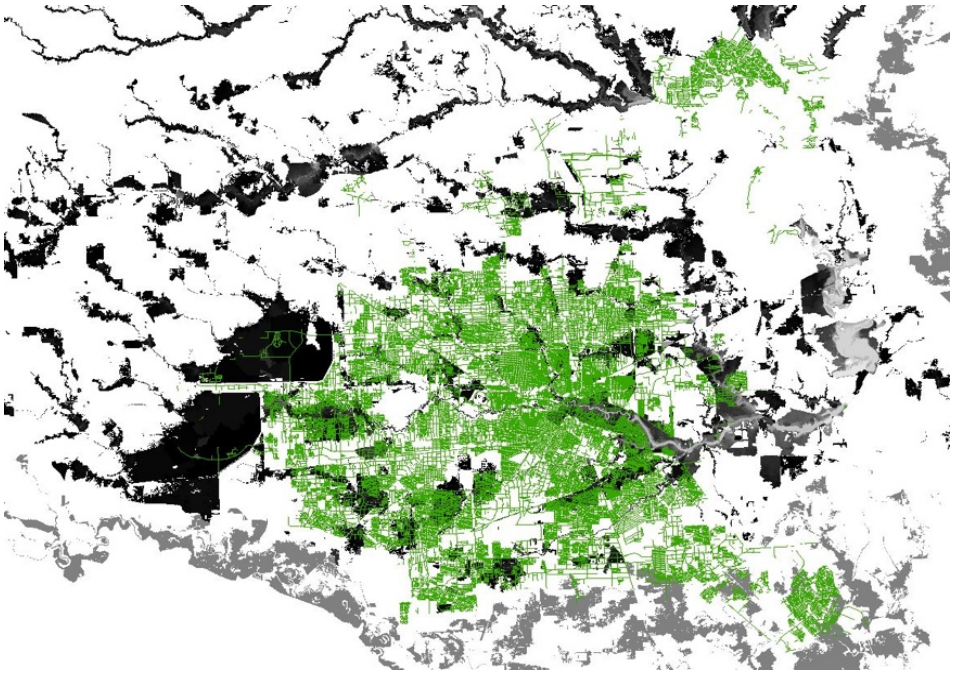

Figure 2. City of Houston street network and flood inundation maps.

4.2. Data Processing in ArcGIS

Detailed street network map and the basin TIFF files were imported into the ArcGIS program to identify the flooded areas. Then the basin TIFF files were converted to polygons using the *Raster to Polygon* tool in the ArcGIS software. Figure 3 shows the polygon layer of the basins. By using the *Intersect Analysis* tool, a new layer containing the affected streets by the Hurricane Harvey was created, as shown in red in Figure 4. After intersecting the flood polygons with the street layer, at the border of polygons, some street segments were found to be flooded only on a part of their length, as depicted in Figure 5. Therefore, it was decided to categorize the street segments flooded

on more than 99.5% of their length as fully flooded segments and the remaining ones as partially flooded. Since the flood raster files were provided as a contour, the raster files were reclassified into one class range raster file using the *Reclassify* function to avoid dividing the length of streets into several objects with shorter lengths when they are located in the borders of contour. After intersecting the flood raster files with the street grid and evaluating the attributes table for flooded segments, it was found that ArcGIS defines a new attribute for the length of the fully and partially flooded segments, called "*Shape_Leng*". The partially flooded streets were determined by defining Equation 13 in the "*Select by Attributes*" section and a new layer for the partially flooded street was created.

$$\frac{Shape\_Length}{Shape\_Leng} < 0.995 \qquad [13]$$

The same procedure in ArcGIS was followed for all the 7 days of flooding. Then the attribute tables were extracted from the resulting layers into Excel format file. After that all the data was assembled in a single spreadsheet for further analysis.

Different columns were considered for each day of flooding to determine the total number of flood days for each street segment. Then the street segments were sorted based on their SectionID. Since a specific SectionID was flooded on different days, they were shown in the separate rows as illustrated in Table 2. To combine the rows for the similar SectionID, the *Consolidate* function in Excel was used to combine the data stored in multiple rows into one row. Also, the total number of flooded days were determined for each street segment. Table 3 shows the resultant data set. A number of 19,682 street segments were discovered to be affected by the flood during the 7 days of the hurricane.

The same procedure was followed for the partially flooded segments. Moreover, the flooded length percentages were calculated by dividing the "*Shape_Leng*" to "*Shape_Length*" for each flooding day. Then the partially flooded street data were matched with the flooded street data by considering the SectionID and using the *VLOOKUP* function in Excel.

The proposed method to identify the road and street sections flooded during a hurricane or other major natural disasters provides fast and with only a few operations the list of fully or partially flooded road or street section. Another benefit is that it doesn't require an assembly of such a list from other sources such as site visits or employee surveys. The major limitation is that it considers a section as being fully or partially flooded based on the contour maps of flooded area. The underlying assumption used is that a pavement structure is flooded when the surrounding area is flooded. This may not be always true, especially for roads and highways that many times are built on an embankment higher that the surrounding ground. Therefore, the proposed methodology is more useful for identifying streets that have been flooded fully or partially; street are built commonly built at a lower elevation than the surrounding ground so that part of the rainwater from the surrounding ground will be collected in the street gutter. In addition, street networks have high number of sections. For road networks, the list of flooded sections may be more accurate if assembled through field visit and employee surveys.

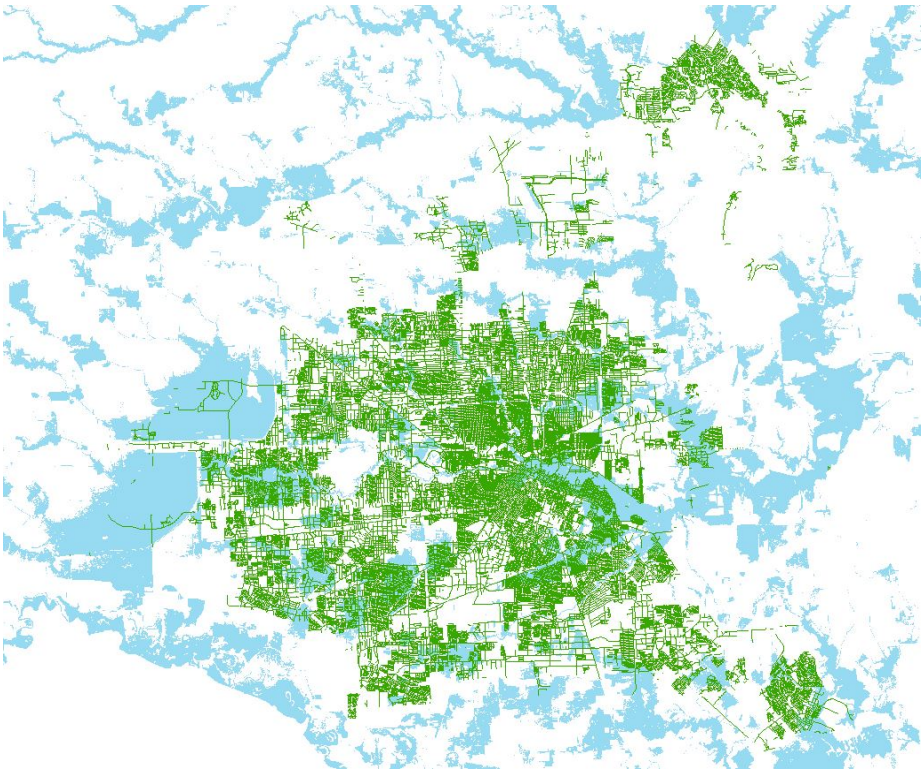

Figure 3. Polygon representation of basins.

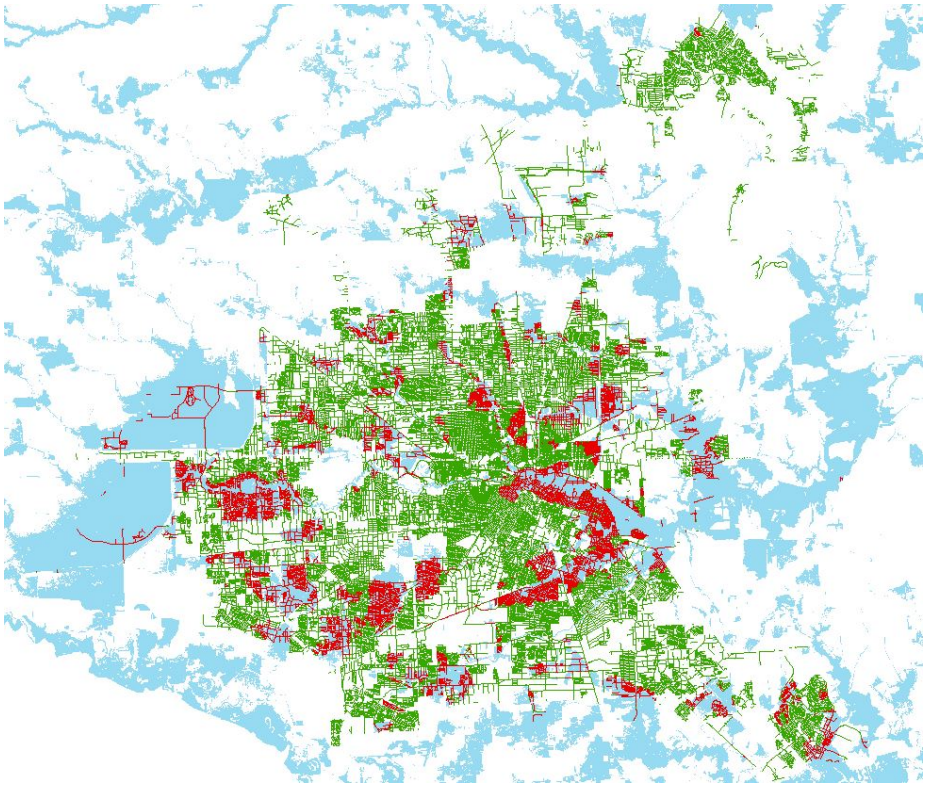

Figure 4. Flooded streets on August 28.

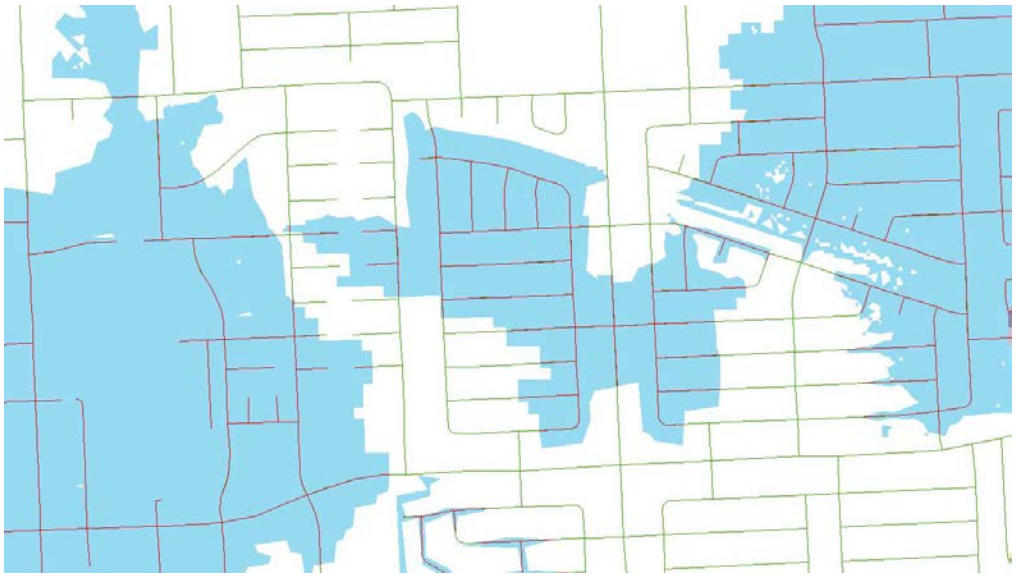

Figure 5. Partially and fully-flooded streets.

Table 2. Flooded pavement sections by days.

SectionID	28-Aug	29-Aug	30-Aug	31-Aug	1-Sep	2-Sep	3-Sep
1027980	X						
1027980		X					
1027980			X				
1032128	X						
1032128		X					
1032128			X				
1032128				X			
1034934	X						
1034934		X					
1046339	X						
1046339		X					
1046339			X				
1046339				X			
1046339					X		
1046339						X	
1046339							X
1060298	X						
1070481	X						
…	…	…	…	…	…	…	…

Table 3. Flooded pavement sections by days – consolidated.

No.	Section ID	28-Aug	29-Aug	30-Aug	31-Aug	1-Sep	2-Sep	3-Sep	Total Days Flooded
1	1002575	X							1
2	1003231	X	X	X	X	X	X	X	7
3	1008087	X	X	X	X	X	X	X	7
4	1008315	X	X	X	X	X	X	X	7
5	1026745	X	X	X	X	X	X	X	7
6	1027980	X	X	X					3
7	1032128	X	X	X	X				4
8	1034934	X	X						2
9	1046339	X	X	X	X	X	X	X	7
10	1060298	X							1
11	1070481	X							1
12	1074915	X	X						2
13	1078238	X	X	X					3
…	…	…	…	…	…	…	…	…	…
19682	1085444	X							1

5. ANALYSIS AND FINDINGS

After organizing the data exported form ArcGIS, it was found that the IRI values were not recorded for the residential streets. In addition, there was no PCI data for major collectors in the available dataset. Therefore, the expected analysis could not be performed on the Houston city street network.

In order to recognize the economic and environmental effects of the Hurricane Harvey on the street network, an example dataset including 19 streets shown in Table 4 was selected. This table was used as input dataset into a new Excel file that is used for data analysis. The Excel file contains three worksheets: Data, Calculation, and Results; they are described in the subsequent sections.

5.1. Data Worksheet

In this worksheet, the data was organized in the following columns: Section ID, Functional Class, Surface Type, Number of lanes, Length of the street (miles), Traffic speed (mph), Traffic Volume, Truck Percentage, Measured IRI and PCI in different years before the hurricane, and Measured IRI and PCI after the Hurricane. The table can be obtained by extracting data from the database containing road or street network distress and performance data. The database should always contain and overall performance index, such as the Pavement Condition Index (PCI) and a roughness index, the International Roughness Index (IRI) being the most common. The dates in which the IRI and PCI were recorded must be entered in the highlighted cells in this sheet, as replicated in Table 4. For the purpose of this study, the measured IRI and PCI from four years were considered, but the worksheet can consider up to five years of PCI and IRI measurements. If desired, the Excel macro can be easily modified to accommodate more than five years of data.

Table 4. Data worksheet.

								4/7/2010	4/14/2013	6/17/2015	8/8/2017	4/7/2010	4/14/2013	6/17/2015	8/8/2017	10/20/2018	10/20/2018
Section ID	Functional Class	Surface Type	Number of Lanes	Length	Traffic Speed (mph)	Traffic Vol.	Truck (%)	Measured IRI 1	Measured IRI 2	Measured IRI 3	Measured IRI 4	Measured PCI 1	Measured PCI 2	Measured PCI 3	Measured PCI 4	Measured IRI after the Hurricane	Measured PCI after the Hurricane
10100	Local Street	PCC	2	0.35	30	70	10	128.4	133.7	143.9	155.0	99	94	88	80	340	68
10101	Collector	PCC	4	1.20	40	100	20	150.0	175.6	305.6	392.4	100	98	89	83	550	69
10102	Local Street	AC	2	0.50	30	70	15	184.5	270.9	400.0	487.4	99	89	77	69	633	55
10103	Local Street	PCC	2	0.40	30	70	15	120.0	356.9	425.1	488.0	100	98	89	70	504	44
10104	Local Street	PCC	2	0.55	30	70	15	293.6	310.6	380.0	423.4	99	98	93	88	626	69
10105	Collector	PCC	4	1.50	40	100	30	178.1	283.1	367.8	374.6	100	98	94	90	478	74
10106	Local Street	AC	2	0.70	35	70	10	261.4	280.4	325.4	357.2	99	94	90	85	550	68
10107	Local Street	AC	2	0.30	35	70	10	281.7	286.0	342.9	400.0	96	91	85	72	548	59
10108	Collector	PCC	4	0.90	45	100	15	296.1	327.8	437.0	486.3	93	78	71	66	625	47
10109	Local Street	AC	2	0.45	35	70	5	279.0	284.4	297.7	384.5	99	92	80	73	521	59
10110	Collector	AC	4	1.40	40	100	30	197.4	350.4	447.0	476.3	99	81	70	65	261	49
10111	Collector	PCC	4	2.00	45	100	25	273.9	330.3	367.9	397.0	99	92	79	72	516	59
10112	Collector	PCC	4	0.60	45	100	20	244.4	255.7	267.7	283.3	100	94	88	83	558	73
10113	Local Street	AC	2	0.60	30	70	5	110.5	147.0	193.1	222.2	99	86	83	75	556	55
10114	Local Street	AC	2	0.80	30	70	15	165.2	193.1	234.8	274.8	100	92	85	79	615	68
10115	Local Street	AC	2	0.40	30	70	10	267.5	308.0	354.0	394.8	100	94	84	74	543	44
10116	Collector	PCC	4	0.50	40	100	20	217.5	273.6	364.6	428.0	100	94	81	70	604	49
10117	Collector	PCC	4	0.50	40	100	25	245.7	287.9	342.7	375.0	100	92	79	75	555	59
10118	Local Street	PCC	2	0.35	30	70	10	128.4	168.7	244.0	273.5	99	94	88	83	570	59

5.2. Calculation Worksheet

To conduct the analysis for each pavement section, data are copied from Data sheet to Calculation sheet, one line at a time, as replicated in Figure 6. In order to compare the effect of the Hurricane Harvey on pavement performance and select the required rehabilitation, the user must input several values: rehabilitation actions, the unit cost trigger value of each action, the discount rate, the cost growth rate. The rehabilitation actions are the action the road or street administration agency considers in the rehabilitation decision three. It is common practice that different rehabilitation actions are used for different pavements structure types (e.g. asphalt, concrete, composite), functional classes and condition levels. The two tables in Figure 7 show highlighted in yellow the values that must be inputted by the user. The discount rate and growth rate should be entered in percentages.

	A	B
25	SectionID	10100
26	Functional Class	Local Street
27	SurfaceType	PCC
28	Number of lanes	2
29	Length	0.35
30	Traffic Speed (mph)	30
31	Traffic Vol.	70
32	Truck (%)	10
33	Measured IRI 1	128.4
34	Measured IRI 2	133.7
35	Measured IRI 3	143.9
36	Measured IRI 4	155.0
37	Measured IRI 5	
38	Measured PCI 1	99
39	Measured PCI 2	94
40	Measured PCI 3	88
41	Measured PCI 4	77
42	Measured PCI 5	
43	Measured IRI after the hurricane	340
44	Measured PCI after the hurricane	65

Figure 6. Pavement section data copied in Calculation sheet.

	A	B	C	D	E
1	Analysis Date	9/17/2019	19.71		
2	Discount Rate (%)	6			
3	Growth rate (%)	2			
4					
5	Functional class	Surface Type	Trigger Values	Rehab Type	Cost per lane*mi
6	Local Street	PCC	75	Diamond Grinding	$ 4,901
7	Local Street	PCC	60	Full Depth Repair	$ 43,453
8	Local Street	PCC	45	Slab Replacement	$ 68,621
9	Local Street	PCC	35	3.0in. HMA Overlay	$ 115,534
10	Local Street	AC	70	Crack filling	$ 1,453
11	Local Street	AC	60	Microsurfacing	$ 30,000
12	Local Street	AC	45	Chip Seal	$ 67,193
13	Local Street	AC	35	2.0in. HMA Overlay	$ 77,023
14	Collector	PCC	75	Diamond Grinding	$ 4,901
15	Collector	PCC	60	Full Depth Repair	$ 43,453
16	Collector	PCC	50	Slab Replacement	$ 68,621
17	Collector	PCC	35	4.0in. HMA Overlay	$ 154,046
18	Collector	AC	75	Crack filling	$ 1,453
19	Collector	AC	60	Microsurfacing	$ 30,000
20	Collector	AC	50	Chip Seal	$ 67,193
21	Collector	AC	35	4.0in. HMA Overlay	$ 154,046

Figure 7. Required input values in the Calculation sheet.

5.2.1. Predicting IRI in Case of No Hurricane

In order to find the effect of the flooding on the condition of the flooded street segments, it is required to develop a performance model. This model could be used to predict the condition of a pavement section if it was not affected by flooding. Many deterministic model forms are available for predicting pavement performance, including straight-line extrapolation, regression, S-shaped curves, polynomial constrained least squares models.

In the example presented, available historical data, including the IRI values in 2010, 2013, 2015, and 2017, were utilized to develop an IRI prediction model for the flooded street segments, The IRI data has been divided into two main categories. The first category is the IRI values before the hurricane (measured in 2010, 2013, 2015 and 2017), and the second category is the measured IRI values in 2018 which has been recorded as a part of the first condition survey after the hurricane. This data set was carefully analyzed to assure that all street segments contain measured IRI values in all three years without showing declines in the IRI values. Segments that showed decreases in IRI values were eliminated. The following second-order polynomial function is selected since it seems to be more reasonable than other model forms:

$$IRI_i = a(T - T_0)^2 + b(T - T_0) + c \qquad [14]$$

In which, T is the year of IRI measurements and T_0 is the reference year (considered as 2009 for this example). Since the date of measurements are in mm/dd/yyyy format the following formula was used to convert them to year and decimal format:

= (YEAR(*date*)+((*date*)-DATE(YEAR(*date*),1,0))/(DATE(YEAR(*date*)+1,1,0)-DATE(YEAR(*date*),1,0)))-2000

The regression coefficients a, b, and c can be determined using Excel Solver. For IRI models other than linear, it is necessary to implement iterative non-linear least squares fitting method. To find the suitable IRI prediction model (best fit), initial regression coefficient values were considered in cells I23 to K23 of the Calculation sheet. Then, as can be seen in Figure 8, using these initial values and the proposed function, the square of differences between calculated values by the model and measured IRIs (square errors) were computed in cells M23 to Q23.

The next step in finding the suitable model is to minimize the value of the Sum of Square Error (SSE), which is described as the following equation:

$$SSE = \sum(y - y_{fit})^2 \qquad [15]$$

Where y is the data point, and y_{fit} is the value of the curve at point y. The example spreadsheet can consider up to five historical performance measurements. Since the Solver cannot be run on a cell including IF function, three scenarios were determined for computing SSE. Therefore, SSE1, SSE2, and SSE3 were defined in cells U23 to W23, in which SSE1, SSE2, and SSE3, respectively, are the sum of square errors correlated with the cases with three, four, and five IRI values recorded before the hurricane. Based on the numbers of recorded IRI measurements, the proper SSE is selected from SSE1 to SSE3 and it is saved in cell T23. In this cell, an IF function is defined, which checks the availability of IRI value in B26 and B27 and copies the relevant SSE in cell T23. Then this value is copied to cell R23 as a Final SSE for the calculation. The Solver is then called to

minimize the final SSE by changing the initial regression values (a, b, and c). Since it is known that the IRI is increasing by the age of the pavement, to ensure the positive slope of the model, a constraint added to the Solver to have "a" as a positive number ($a \geq 0$).

	H	I	J	K	L	M	N	O	P	Q	R	S	T	U	V	W
22	IRI	a	b	c	R-square	Dif1	Dif2	Dif3	Dif4	Dif5	Final SSE	TSS	SSE	SSE 1	SSE 2	SSE 3
23		0.39	-0.1	127.8	0.997	2.68E-02	4.43E-01	6.06E-01	7.71E-02	2.25E+07	1.15E+00	4.15E+02	1.15E+00	1.08E+00	1.15E+00	2.25E+07
24				c'	Calc. Value	Squared Error										
25				304.12	340.0	0.00										

Figure 8. Calculation of regression coefficients for the IRI prediction model.

The coefficient of determination (R^2) is defined as following equation:

$$R^2 = 1 - \frac{SSE}{TSS} \quad [16]$$

In which TSS is the Total Sum of Square which is calculated as:

$$TSS = \sum(y - y_{mean})^2 \quad [17]$$

Where y_{mean} is the average value of data points. Since the value of TSS depends on the numbers of measured data points, the following formula was written in cell S23 to calculate TSS:

= (B33-AVERAGE(B33:B37))^2+(B34-AVERAGE(B33:B37))^2+(B35-AVERAGE(B33:B37))^2+IF(B36>0,(B36-AVERAGE(B33:B37))^2,0)+IF(B37>0,(B37-AVERAGE(B33:B37))^2,0)

Having the Final SSE and TSS, respectively in cells R23 and S23, the R^2 was calculated in cell L23 by entering the following formula:

= 1-R23/S23

As can be seen in Figure 8, for the first road section, the Solver calculated a, b, and c, as 0.46, -0.2, and 128 respectively. Therefore, the prediction model for IRI is as following:

$$IRI_i = 0.39(T - 9)^2 - 0.1(T - 9) + 127.8 \quad [18]$$

The IRI for 2018 expected if the street section would not have been affected by the flooding is calculated using Equation 18 in cell B35, as follows:

= I23*(H1-9)^2 + J23*(H1-9) + K23

As shown in Figure 9, to show the goodness of fit of the developed IRI model for each pavement section, the calculated R^2 are copied to cell B46 as an output of the analysis.

Standard error of the regression represents the accuracy of the prediction. The standard error (SE) of the y values is calculated as:

$$SE = \sqrt{\frac{\sum(y - y_{fit})^2}{df}} \quad [19]$$

In which df is the degree of freedom. The df is defined as the number of data point minus the number of parameters in the function. Therefore, to compute the SE the following formula was written in cell B47:

= SQRT(R23/(COUNT(B33:B37)-1))

As can be seen in Figure 9, the predicted IRI in 2018 in case of no hurricane, R^2, and the standard error for this pavement section were calculated as 163.67, 0.997, and 0.62, respectively.

	A	B
45	Predicted IRI	163.67
46	R-Squared (R2) for IRI	0.997
47	Standard Error for IRI	0.62
48	Delta IRI	176.33

Figure 9. Predicted IRI, R2, and the standard error.

5.2.2. Computation of IRI Difference

To find the impact of the flooding on increasing the IRI value, the difference between measured and predicted IRI after the hurricane is calculated in cell B48 (Figure 9).

5.2.3. Predicting PCI in Case of No Hurricane

Similar to the IRI, a model for predicting PCI was developed using a second order polynomial function as follows:

$$ICI_i = m(T - T_0)^2 + n(T - T_0) + o \qquad [20]$$

In which, T is the year of PCI measurements, and T_0 is the reference year (2009), and m, n, and o are the regression coefficients.

To find the best fit for the model, the similar procedure was followed. As can be seen in Figure 10, initial regression coefficient values were considered in cells I28 to K28 of the Calculation sheet. Then, using these initial values and the proposed function, the square differences between of measured and predicted PCI were computed in cells M28 to Q28. As explained in the previous step, three scenarios for SSE were defined, and SSE1, SSE2, and SSE3 were computed in cells U28 to W28. Based on the numbers of PCI measurements, the proper SSE is selected from SSE1 to SSE3, and it is saved in cell T28. Then this value is copied to the cell R28 as a Final SSE for the calculation. Further, the Solver is used to minimize the Final SSE by changing the initial regression values (m, n, and o). Since it is known that the PCI is decreasing with the age of the pavement, to ensure the negative slope of the model, the "m" coefficient was constraint as a negative number ($m \leq 0$). Then, TSS is calculated to find R^2. The following formula was written in cell S28 to calculate TSS:

= (B38-AVERAGE(B38:B42))^2+(B39-AVERAGE(B38:B42))^2+(B40-AVERAGE(B38:B42))^2+IF(B41>0,(B41-AVERAGE(B38:B42))^2,0)+IF(B42>0,(B42-AVERAGE(B38:B42))^2,0)

The R^2 was calculated by entering the following formula in cell L28:

= 1-R28/S28

	H	I	J	K	L	M	N	O	P	Q	R	S	T	U	V	W
27	PCI	m	n	o	R-square	Dif1	Dif2	Dif3	Dif4	Dif5	Final SSE	TSS	SSE	SSE 1	SSE 2	SSE 3
28		-0.35	0.5	98.8	0.998	1.54E-02	2.52E-01	3.44E-01	4.37E-02	1.68E+07	6.55E-01	2.69E+02	6.55E-01	6.11E-01	6.55E-01	1.68E+07
29				o'	Calc. Value	Squared Error										
30				93.72	65.00	0.00										

Figure 10. Calculation of regression coefficients for the IRI prediction model.

As shown in Figure 10, the Solver calculated for this pavement section m, n, and o, as -0.26, -0.4, and 99.6 respectively. Therefore, the prediction model for PCI is as following:

$$PCI_i = -0.35(T-9)^2 + 0.5(T-9) + 98.8 \qquad [21]$$

Thus, the expected PCI in 2018 if the street section would not have been affected by the hurricane is calculated using Equation 21 in cell B49 as:

= I28*(H1-9)^2+J28*(H1-9)+K28

As shown in Figure 11, R^2 was copied in cell B50 and the SE of the prediction model was calculated by writing the following formula in cell B51:

= SQRT(R28/(COUNT(B38:B42)-1))

	A	B
49	Predicted PCI	70
50	R-Squared (R2) for PCI	0.998
51	Standard Error for PCI	0.47

Figure 11. Predicted PCI, R^2, and the standard error.

5.2.4. Current Condition of the Pavement Section

In pavement management, when the PCI drops to a preselected trigger value, rehabilitation is planned. To make a decision for the trigger value and the proper rehabilitation type, it is necessary to find the current condition of the pavement. Therefore, the PCI of the pavement section at the time of performing analysis should be predicted.

If flooding affects the pavement section, its PCI value after the flooding should be lower than the PCI value predicted by the model from the data recorded before the flooding. Since the prediction model in Equation 21 could not consider this change in PCI, another PCI prediction model should be developed by considering the measured PCI value after the hurricane. To find this PCI prediction model, it was assumed that it follows a trend model parallel to the prediction model with a different intercept, as illustrated by the dash-dot line in Figure 12.

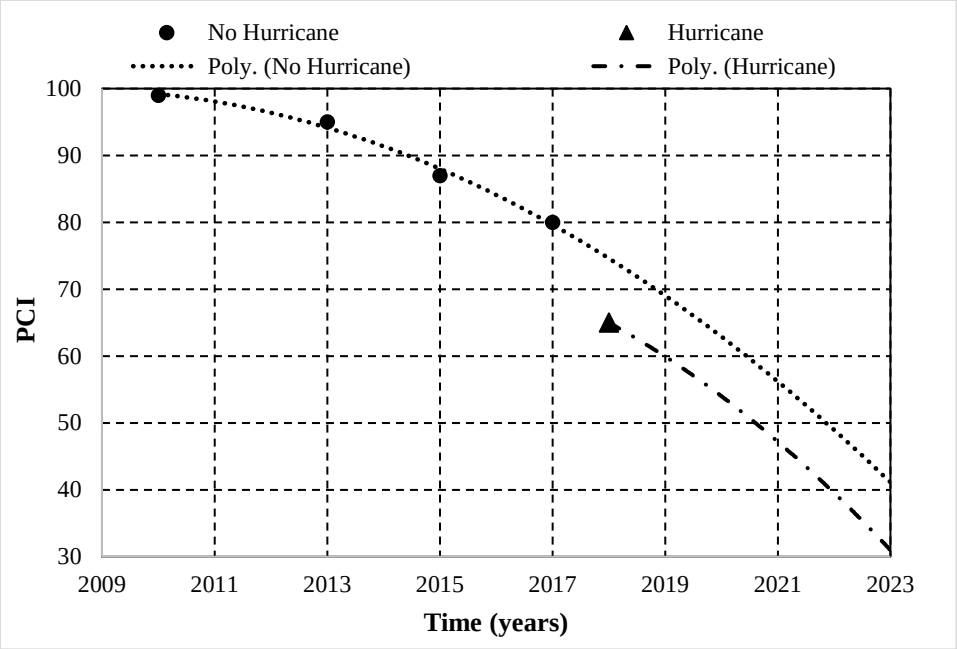

Figure 12. PCI prediction model after the hurricane.

To find this prediction model, a new intercept for the former model should be computed such that the model passes the measured PCI after the hurricane in the measurement year. For the presented example, as illustrated in Figure 12, the PCI in 2018 after the hurricane was measured as 65. Therefore, the following equation should be solved to find the new intercept:

$$65 = -0.35(T-9)^2 + 0.5(T-9) + o'$$

In which, T is the year of PCI measurement, and o' is the intercept of the new model. The year of measurement (2018) is available in the cell H1. To find o', an initial value was entered in cell K30, and the following formula was written in cell L30:

$$= -0.35*(B1-9)\text{^}2 + 0.5*(B1-9) + K30$$

This equation should produce the measured PCI value of 65, so the square error of the outcome of the formula and the value of 65 was computed in cell M30, as following:

$$= (B44-L30)\text{^}2$$

The Excel Solver was run to minimize the value of cell M30 by changing the value in cell K30. The computed o' was found as 89.45 as can be seen in the Figure 13. Therefore, the PCI prediction model for this pavement section after the hurricane is as following:

$$PCI = -0.26(T - T_0)^2 - 0.1(T - T_0) + 91.39 \qquad [22]$$

	H	I	J	K	L	M
27	PCI	m	n	o	R-square	Dif1
28		-0.35	0.5	98.8	0.998	1.54E-02
29				o'	Calc. Value	Squared Error
30				93.72	65.00	0.00

Figure 13. Calculation of the PCI model after the hurricane.

Having the PCI prediction model, the PCI of the pavement section at the time of analysis can be calculated. To do so, the date of analysis is automatically picked by entering =TODAY() function in cell B1 as mm/dd/yyyy format. Then, in cell C1 the date was converted to the year and decimal format using the following formula:

= (YEAR(B1)+((B1)-DATE(YEAR(B1),1,0))/(DATE(YEAR(B1)+1,1,0)-DATE(YEAR(B1),1,0)))-2000

As an example, this formula converts the date of 9/17/2019 to 19.71. Then this date is used to calculate the PCI of the pavement section at the time of using the following formula in cell B52:

= I28*(C1-9)^2+J28*(C1-9)+K30

5.2.5. Selection of Rehabilitation Type and its Unit Cost

To find the proper rehabilitation type and cost of rehabilitation, the input values in Figure 9 are utilized to generate a separate table containing useful suitable trigger value, rehabilitation type, and cost (shown in Figure 14).

	O	P	Q	R	S
12	Functional cl.	Surface Type	Trigger value	Rehab Type	Cost
13	Local Street	PCC	45	Slab Replacement	$ 68,621
14	Local Street	AC	45	Chip Seal	$ 67,193
15	Collector	PCC	50	Slab Replacement	$ 68,621
16	Collector	AC	50	Chip Seal	$ 67,193
17			45	Slab Replacement	$ 68,621

Figure 14. Selection of trigger value, rehabilitation type, and cost.

In this table, the suitable trigger values for each functional class and surface type are selected by comparing the current PCI value of the pavement section, calculated in the previous section, with the trigger values in Figure 6. The suitable trigger value for the pavement section was selected as the highest value smaller than the current PCI. For a PCC local street, the following formula was written in cell Q13:

= IF($B$52>=C6,C6,IF($B$52>=C7,C7,IF($B$52>=C8,C8,C9)))

This formula compares the current PCI value calculated in cell B52 with the trigger values in cells C6 to C9 to have the current PCI bigger than the trigger value, then it selects that trigger value as a suitable trigger value for this pavement section. Similar formulas were entered in cells Q14 to Q16 for other types of streets.

Cell R13 contains the following formula in order to select the rehabilitation type for a PCC local street:

= IF(Q13=C6,D6,IF(Q13=C7,D7,IF(Q13=C8,D8,D9)))

In this formula the selected trigger value in the previous step was compared to the trigger values in cells C6 to C8, and finds the relevant rehabilitation type for the selected trigger value. Similar formulas were used in cells R14 to R16 for other types of streets.

Cell S13 calculates the cost of the selected rehabilitation type for a PCC local street with the formula:

= VLOOKUP(R13,D6:E9,2,FALSE)

This formula seeks the selected rehabilitation type written in cell R13 in cells D6 to D9 and finds the relevant cost. Similar formulas were written in cells S14 to S16 for other types of streets.

In order to find the trigger value of the current pavement section in the analysis, the following formula was used in cell Q17:

= VLOOKUP(B27,IF(B26=O13,P13:S14,P15:S16),2,FALSE)

This formula looks for the surface type of the pavement available in cell B27, in the green and the red table arrays shown in Figure 15. As shown in this figure, if the functional class of the pavement section from the cell B26 matches the functional class in cell O13, the green table array (P13 to S14) is used; Otherwise the red table array (P15 to S16) is used. Then the correlated value from the second column of the green table array is copied to cell Q17 as a final trigger value.

	O	P	Q	R	S
12	Functional cl.	Surface Type	Trigger value	Rehab Type	Cost
13	Local Street	PCC	45	Slab Replacement	$ 68,621
14	Local Street	AC	45	Chip Seal	$ 67,193
15	Collector	PCC	50	Slab Replacement	$ 68,621
16	Collector	AC	50	Chip Seal	$ 67,193
17			45	Slab Replacement	=VLOOKUP(

Figure 15. Table arrays used in Vlookup function.

Similarly, the final rehabilitation type and the relative cost are selected using the following formulas, which copy the relevant value to cells R17 and S17 respectively.

= VLOOKUP(B27,IF(B26=O13,P13:S14,P15:S16),3,FALSE)

= VLOOKUP(B27,IF(B26=O13,P13:S14,P15:S16),4,FALSE)

As shown in Figure 15, the trigger value of 45 was selected to perform the slab replacement operation at a cost of $68,621. The type of rehabilitation is copied to cell B53.

5.2.6. Prediction of the Year of Rehabilitation

Since the flooding degrades the condition of the pavement, the rehabilitation needs to be performed earlier than what is predicted by the PCI model from past values, as illustrated in Figure 16.

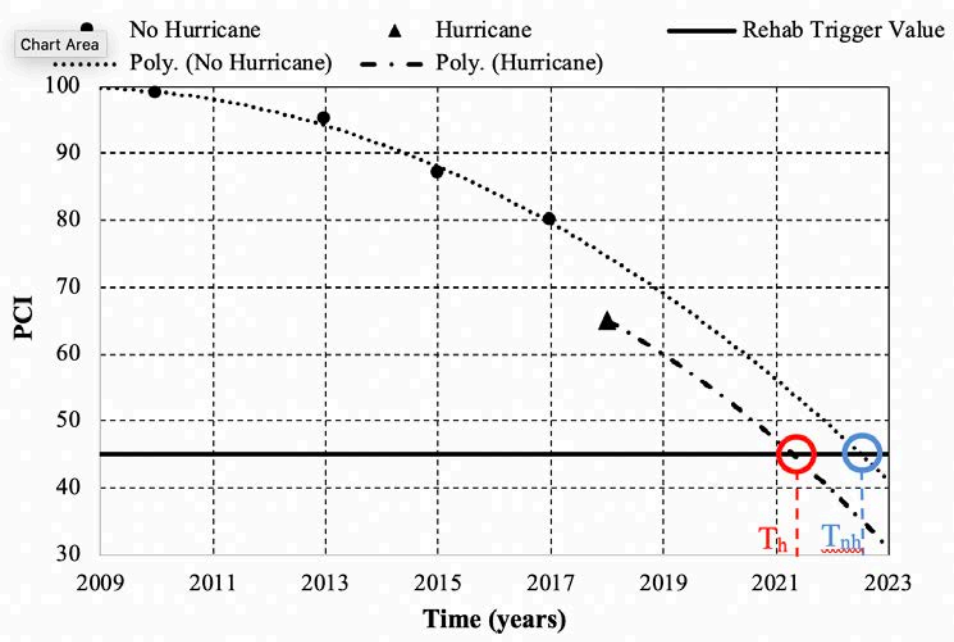

Figure 16. Difference in year of rehabilitation in case of hurricane and no hurricane.

As can be seen in this figure, if the hurricane would not have happened, the PCI would reach the trigger value for rehabilitation later (in year T_{nh}). However, the decrease in PCI value due to the hurricane yields the need for rehabilitation earlier (in year T_h).

T_{nh} can be calculated using the proposed prediction model in Equation 21. Therefore, the following formula was written in cell F54:

= I28*(E54-9)^2+J28*(E54-9)+K28

This formula should produce the trigger value (45 in this example), so, as shown in Figure 17, the square error of the outcome of the formula and the trigger value was computed in cell G54. An initial value for year of rehabilitation was considered in cell E54. Then, the Excel Solver was run to minimize the value of cell G54 by changing the value in cell E54. The computed T_{nh} is in yy format. It was converted to yyyy format using the following formula in cell D54:

= E54+2000

The exact date of rehabilitation was found in mm/dd/yyyy format using the following formula:

= DATE(INT(D54),1,MOD(D54,1)*(DATE(INT(D54)+1,1,1)-DATE(INT(D54),1,1)))

Since it is possible for some pavement section that the measured PCI after flooding is less than the smallest trigger value, the date of rehabilitation cannot be calculated. Immediate reconstruction must be considered. Thus, the following formula was written in cell B54 to account for this particular case:

= IF(E54>=C1,DATE(INT(D54),1,MOD(D54,1)*(DATE(INT(D54)+1,1,1)-
DATE(INT(D54),1,1))),"Already Failed")

This formula compares the predicted date of rehabilitation (E54) to the date of analysis (C1). If the date of rehabilitation is earlier than the date of analysis, the result will show “Already Failed”. Otherwise, it shows the T_{nh} in mm/dd/yyyy format in cell B54.

The year of rehabilitation after flooding (T_h) was calculated using the proposed prediction model in Equation 22 with the following formula in cell F55:

= I28*(E55-9)^2+J28*(E55-9)+K30

A similar procedure was followed for finding T_h in cell B55 (Figure 17).

	A	B	C	D	E	F	G
53	Type of rehab	Slab Replacement					Squared Error
54	Predicted yr. rehab with no hurricane (Tnh)	2/21/2022		2022.14	22.14	45	0.00
55	Predicted yr. rehab with hurricane (Th)	7/17/2021		2021.54	21.54	45	0.00
56	Delta T (yr.)	0.60					

Figure 17. Calculated the yearly rehabilitations.

5.2.7. Impact of the Hurricane on Time of Rehabilitation

As observed in the previous section, one of the impacts of the hurricane is changing the time of rehabilitation. This change in time of rehabilitation (ΔT) can be calculated by subtracting T_h from T_{nh}. ΔT was calculated in cell B56 by subtracting E55 from B54 (Figure 17). If the calculated value of ΔT is positive, this means that T_h should happen earlier than T_{nh}.

5.2.8. Prediction of IRI at the Time of Rehabilitation

In order to find the IRI of pavement section at T_h and T_{nh}, IRI prediction models should be used. The IRI prediction model in case of no hurricane was developed in Equation 18. Since the deterioration of the pavement section due to the hurricane leads to a sudden increase in the IRI, another IRI model is needed for the predication of IRI after the flooding. To find this IRI prediction model, it was assumed that this model is parallel to the IRI prediction model developed from the data before the flooding (Equation 18) but with a different intercept, as shown in red color in Figure 18.

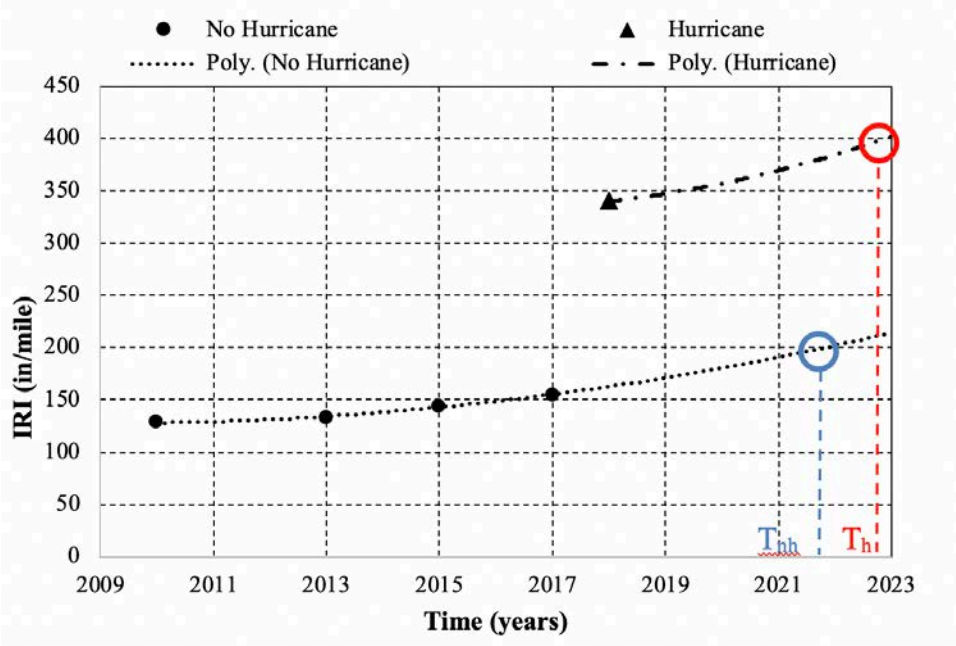

Figure 18. IRI prediction models and years of required rehabilitation.

For the presented example as shown in cell B43 (Figure 6), the measured IRI in 2018 after the hurricane was 340. Therefore, the following equation should be solved to find the new intercept.

$$340 = 0.39(T\text{-}9)^2 - 0.1(T\text{-}9) + c'$$

In which, T is the year of IRI measurement, and c' is the intercept of the new model. The year of measurement (2018) is available in cell H1. To find the c', an initial value was entered in cell K25. Then, the following formula was written in cell L25.

= I23*(H1-9)^2+J23*(H1-9)+K25

This equation should produce the measured IRI value of 340, so the square error of the result of formula and the measured IRI value of 340 was computed in cell M25. Then, the Excel Solver was run to minimize the value of cell M25 by changing the value in cell K25. The computed c' was found to be 304.12 (Figure 19). The model that predicts the IRI prediction after hurricane becomes:

$$IRI_i = 0.39(T - T_0)^2 - 0.1(T - T_0) + 304.12 \qquad [23]$$

	H	I	J	K	L	M
22	IRI	a	b	c	R-square	Dif1
23		0.39	-0.1	127.8	0.997	2.68E-02
24				c'	Calc. Value	Squared Error
25				304.12	340.0	0.00

Figure 19. Calculation of the new intercept for IRI model.

The IRI of the pavement section at T_{nh} and T_h were computed using Equations 18 and 23, in cells B57 and B58, respectively (Figure 20).

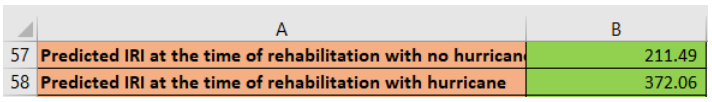

	A	B
57	Predicted IRI at the time of rehabilitation with no hurrican	211.49
58	Predicted IRI at the time of rehabilitation with hurricane	372.06

Figure 20. Predicted IRI at time of rehabilitation.

5.2.9. Z-score of PCI Prediction

A common assumption for a regression model is error follows a normal distribution. For linear regression this can be checked. It is not possible for PCI or the IRI models developed here since the models are derived from a very small number of observations. When a historical condition survey data is available for many years, it is possible to determine if the hurricane had any statistical effect on the PCI by calculating the Z-score using the formula:

$$z = \frac{y_m - y_p}{SE} \qquad [24]$$

in which y_m is the PCI value measured after the flooding, y_p is the predicted value of the PCI, and SE is the standard error. The difference between the measured and predicted PCI is shown in red in Figure 21. The predicted PCI value at the time of measurement can be calculated using Equation 21. To do so, following formula was entered in cell D59:

= I28*(H1-9)^2+J28*(H1-9)+K28

Then, following formula was used in cell B59 to calculate the Z-score:

= (B44-D59)/B51

By considering probability of 0.05, if the calculated Z-score is more than -1.64, it can be considered from statistical point of view that the hurricane had a significant effect on the PCI. Otherwise, this decrease in PCI is close to the expected deterioration of the pavement without the flooding. The formula in cell B60 (Figure 22) compares the calculated the Z-score in cell B59 with the critical value:

= IF(B59<NORM.INV(0.05,0,1),"Yes","No")

If the Z-score is bigger than critical value, the text “Yes” is in cell B60.

The Excel macro can also be used to identify the pavement structures with better resilience to the flooding by grouping sections based on the flooding duration (no flooding, single and multiple day flooding) and on design features such as pavement type, functional class, age or time from the most recent resurfacing or reconstruction, subgrade soil type, traffic volume and layer thickness. In the case of networks with large number of sections, grouping done based on multiple criteria can allow detailed comparison and identification of design feature with more impact on the resiliency to flooding. ANOVA and MANOVA technique can be used to compare the Z-score values calculated for sections in different groups.

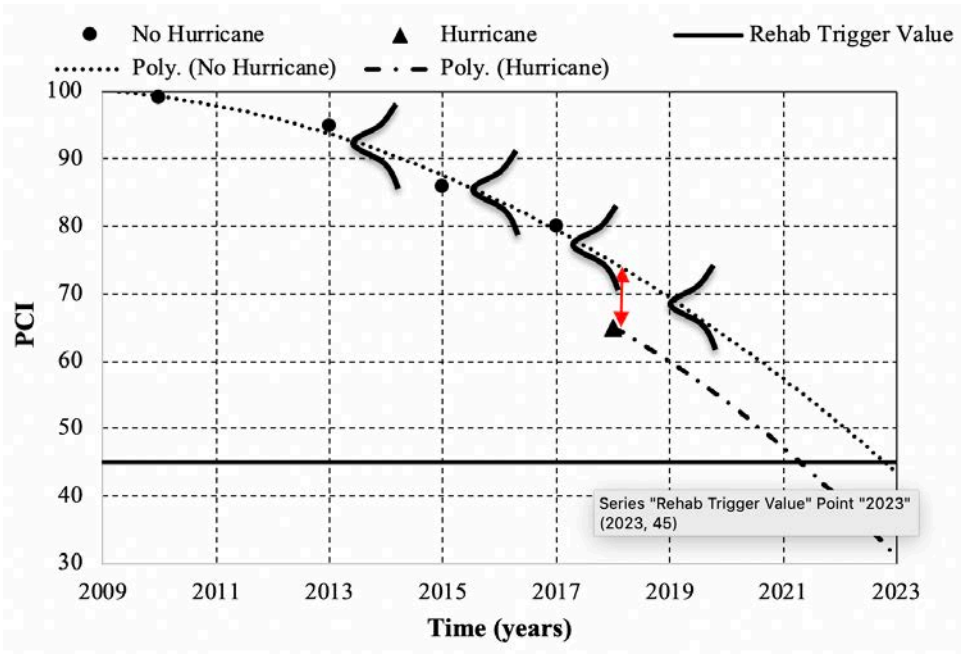

Figure 21. Determination of statistical effect of hurricane on PCI.

	A	B
59	Z-value of PCI	-10.91
60	Statistical effect	Yes

Figure 22. Predicted IRI at time of rehabilitation.

5.3. Estimation of the Effects of Hurricanes on the Entire Road/Street Network

5.3.1. Estimation of the Increase in Rehabilitation Costs

Since the flooding damages pavement structures, the rehabilitation actions need to be done earlier than if the flooding had not happened. Therefore, the rehabilitate costs would happen earlier than if the flooding would had not occurred. To find the difference between the discounted rehabilitation costs, now occurring at a time T_h instead of at the time T_{nh}, the cost of two rehabilitations in the year when they took place is predicted using the following formula:

$$Total\ cost\ of\ rehabilitation = L * n * C * (1 + g)^T \qquad [25]$$

where:
L= the length of the pavement section (mi);
n= number of the lanes;
C= cost of rehabilitation per lane*mile ($)
g = growth rate (%); and
T= time to the rehabilitation (yr).

The cost of the rehabilitation type can be found in the tables shown in Figure 23, which is the current cost of rehabilitation. Using the growth rate, this cost was changed to its value in the years

of rehabilitation. In cells B61 and B62, the predicted rehabilitation costs at times T_h and T_{nh} were calculated as:

= B29*B28*S17*(1+B3/100)^(E54-C1)

Since it is possible that the pavement section under analysis has a predicted rehabilitation date, $T_{nh,}$ that is earlier than the date of analysis (given in cell C1), reconstruction should be considered. Thus, the following formula was written in cell B61 to account for this particular case:

= IF(E54>=C1,B29*B28*S17*(1+B3/100)^(E54-C1),"Reconstruction")

A similar procedure was followed for computing the rehabilitation cost at time T_h in cell B62. The rehabilitation costs at time T_h and T_{nh}, discounted to the date of analysis is done using the following equation:

$$PV = \frac{FV}{(1+r)^i} \quad [26]$$

In which PV is present value, FV is future value, r is the discount rate, and i is the time period. The future value is the total cost of rehabilitations computed in cells B61 and B62. The discount rate can be found in cell B2, and the time period is the difference between the predicted date of rehabilitation and the date the analysis is performed. Therefore, the net present value for each of the two rehabilitations scheduled, at T_{nh} and T_h are calculated in cells E63 and E64 (Figure 23), respectively, as:

= B61/(1+B2/100)^(E54-C1)

= B62/(1+B2/100)^(E55-C1)

Since it is possible that a pavement section might have a predicted rehabilitation date earlier than the day of analysis, the following formula was written in cell B63 to account for this particular case:

= IF(E54>=C1,B61/(1+B2/100)^(E54-C1),"N/A")

This formula compares the predicted date of rehabilitation (E54) to the date of analysis (C1). If the rehabilitation date occurs before the analysis date, the net present value cannot be calculated, and it shows as “N/A” in cell B63. A similar formula was entered in cell B64 for computing the total cost of rehabilitation at T_h. The difference between the costs of performing rehabilitation at T_{nh} and T_h was represented in cell B65 as Delta cost. As explained earlier, the cost analysis cannot be performed on a pavement section which has failed before the analysis date, so the following formula was written in cell B65:

= IF(E54>=C1,IF(E55>=C1,B64-B63,"N/A"),"N/A")

This formula calculates the delta cost by subtracting B63 from B64 when T_{nh} and T_h are future values in compare to the date of analysis. Otherwise, the difference in discounted costs cannot be estimated and “N/A” is shown in cell B65.

	A	B
61	Total Cost of rehab at Tnh	$ 50,405
62	Total Cost of rehab Th	$ 49,808
63	NPV - rehab at Tnh	$ 43,744
64	NPV 2 - rehab at Th	$ 44,769
65	Delta Cost	$ 1,025

Figure 23. Difference in rehabilitation costs.

5.3.2. Estimation of the Increase in Fuel Consumption

Flooding damages pavement structures and increases the IRI and therefore increases user vehicle costs. Studies indicated that an increase in IRI of 60 to 300 in/mile leads to a rise in fuel consumption of 3% to 5% *(19)*. Chatti et al. studied the effect of roughness on fuel consumption. They considered of five different types of vehicles (Medium car, Van, SUV, Light truck, and Articulated truck) in three different speeds (35, 55, and 70 mph) *(19)*. For the purpose of this research, their results for car and articulated truck were considered (Table 5). It was assumed that all cars use gasoline while all trucks use diesel fuel. The approach can be modified if a more refined vehicle classification is *d*.

Table 5. Effect of roughness on fuel consumption (mpg) *(19)*.

Speed (mph)	Vehicle	IRI (in/mile)					
		63.36	126.72	190.08	253.44	316.8	380.16
35	Car	33.53	32.56	31.94	31.05	30.48	29.68
35	Truck	8.60	8.43	8.27	8.04	7.89	7.75
55	Car	28.21	27.39	26.86	26.12	25.64	24.96
55	Truck	5.26	5.15	5.10	5.01	4.96	4.87
70	Car	21.81	21.38	20.77	20.38	20.01	19.47
70	Truck	3.58	3.55	3.51	3.45	3.41	3.38

The fuel consumption in gallons per mile travelled is given in Table 6 for cars and trucks at each of the three speeds, along with the slope of the linear fit between the fuel consumption and the IRI. Table 6 shows that these slopes increase when the speed of the vehicle increases. Therefore, a second order polynomial model relating the increase in fuel consumption per increase in unit IRI (in/mile) at a given vehicle speed (mph) was estimated separately for cars and trucks. These values are given in Table 7.

Table 6. Increase in fuel consumption (10^{-3} gallons per mile) due to change in IRI.

Speed (mph)	Vehicle	IRI (in/mile)						Slope (10^{-3} gal/mile per IRI unit)
		63.36	126.72	190.08	253.44	316.8	380.16	
35	Car	29.82	30.71	31.31	32.21	32.81	33.69	1.196E-02
55	Car	35.45	36.51	37.23	38.28	39.00	40.06	1.425E-02
70	Car	45.85	46.77	48.15	49.07	49.98	51.36	1.717E-02
35	Truck	116.28	118.62	120.92	124.38	126.74	129.03	4.130E-02
55	Truck	190.11	194.17	196.08	199.60	201.61	205.34	4.598E-02
70	Truck	279.33	281.69	284.90	289.86	293.26	299.40	6.313E-02

Table 7. Parameters for the increase in fuel consumption model.

Parameter	Car	Truck
a	10.02	30
b	0.005	0.0786
c	0.00134	0.005228
R^2	0.996	0.935

The increase in fuel consumption due to the increase in the IRI caused by flooding, Δgal_IRI , can be therefore computed as:

$$\Delta gal\_IRI = 10.02 + 0.005 * Speed + 0.00134 * Speed^2 \quad [27]$$

$$\Delta gal\_IRI = 30 + 0.0786 * Speed + 0.005528 * Speed^2 \quad [28]$$

The increase in fuel consumption due to the increase in the IRI caused by flooding, Δgal_IRI , is computed in 10^{-6} gallons per unit IRI (in/mile) per vehicle, per mile. The Speed is measured in miles per hour.

To compute this increase in fuel consumption, the change in IRI of two cases, with hurricane and no hurricane, during the timeframe between T_h and T_{nh} should be considered, as shown in Figure 24. Since two IRI models are parallel, the delta IRI is constant number as calculated in cell B48. Therefore, this area can be calculated by following equation:

$$Area = \Delta IRI * \Delta T = B48 * B5 \quad [29]$$

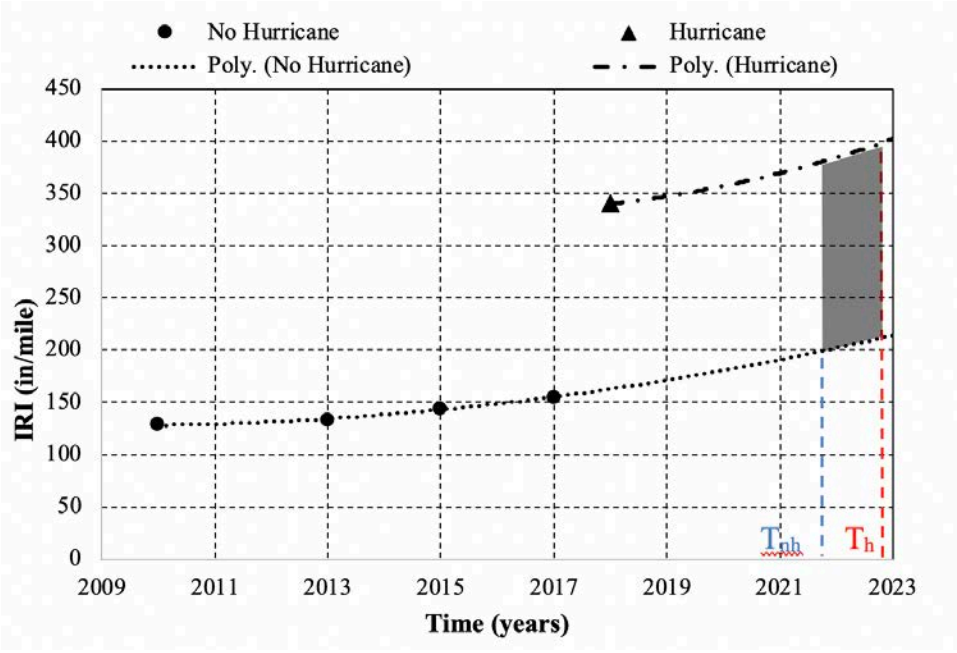

Figure 24. Total change in IRI during in rehabilitation time.

As shown in Figure 25, the total increase in the gasoline consumption considering the car traffic volume, length of section, ΔIRI and ΔT is calculated for the example street section in cell B66 as:

= ((1-B32/100)*B31)*B29*(B48*B56)*J50*(10^-6)*365

In which B31 is traffic volume, B32 is truck percentage, and N49 is extra gas consumption (gal/mi). Similarly, the total increase in diesel consumption is computed in the cell B67.

= (B32/100)*B31*B29*(B48*B56)*K50*(10^-6)*365

	A	B
66	**Increase in gasoline consumption (gallon)**	9.72
67	**Increase in diesel consumption (gallon)**	3.52

Figure 25. Increase in gasoline and diesel consumption.

5.3.3. Estimation of the Increase in CO_2 Emission

The increase in fuel consumption can be used to estimate the increase in CO_2 emission. The amount of CO_2 created from burning one gallon of fuel depends on the amount of carbon in the fuel. Typically, more than 99% of the carbon in fuel is emitted as CO_2 when the fuel is burnt. Very small amounts are emitted as hydrocarbons and carbon monoxide, which are converted to CO_2 relatively quickly in the atmosphere. Carbon content varies by fuel, and some variation within each type of fuel is normal (20). The U.S. Environmental Protection Agency (EPA) provided an average carbon content values to estimate CO_2 emissions. Burning one gallon of gasoline or diesel produce 8.887 and 10.180 kilograms of CO_2, respectively *(20)*. Therefore, these values are used to calculate the effect of the flooding on the increase in CO_2 emission. The table shown in Figure 26 was constructed for this purpose if the user desires to use different values.

	I	J
52	Fuel type	Co2 (Kg/gallon)
53	Gas	8.887
54	Diesel	10.180

Figure 26. CO_2 emission from burning one gallon of gas and diesel.

The following formula was used in the cell B69 to find the increase in CO_2 emission due to the flooding:

= J53*B66+J54*B67

As shown in Figure 27, this is calculated in cell C68 for each road or street section, but it can be calculated only as the total increase in CO_2 emission due to flooding after the total volumes of gasoline and diesel fuel are added up for all sections.

	A	B
45	Predicted IRI	163.67
46	R-Squared (R2) for IRI	0.997
47	Standard Error for IRI	0.62
48	Delta IRI	176.33
49	Predicted PCI	70
50	R-Squared (R2) for PCI	0.998
51	Standard Error for PCI	0.47
52	PCI as of Today	59
53	Type of rehab	Slab Replacement
54	Predicted yr. rehab with no hurricane (Tnh)	2/21/2022
55	Predicted yr. rehab with hurricane (Th)	7/17/2021
56	Delta T (yr.)	0.60
57	Predicted IRI at the time of rehabilitation with no hurricane	192.91
58	Predicted IRI at the time of rehabilitation with hurricane	363.34
59	Z-value of PCI	-10.91
60	Statistical effect	Yes
61	Total Cost of rehab at Tnh	$ 50,386
62	Total Cost of rehab Th	$ 49,789
63	NPV - rehab at Tnh	$ 43,777
64	NPV 2 - rehab at Th	$ 44,802
65	Delta Cost	$ 1,026
66	Increase in gasoline consumption (gallon)	9.72
67	Increase in diesel consumption (gallon)	3.52
68	Increase in CO2 emission (Kg)	122

Figure 27. Output of analysis.

5.4. The Sample Excel Macro

Since the same procedure, discussed in Subsections 3.2 and 3.3 must be followed for every flooded road or street section, an Excel macro was developed to analyze every pavement section available in the Data worksheet. The developed Macro code is presented in the Appendix A.

The developed macro does the following operations, in their respective order:

1. Selects and copies the data available in cells A3 to T3 of the Data worksheet.
2. Transposes and pastes the values in the cells B25 to B44 of the Calculation worksheet.
3. Runs the Solver to minimize the value in the cell R23 by changing I23 to K23, by having I23>0 as a constraint.
4. Runs the Solver to minimize the value in the cell M25 by changing K25.
5. Runs the Solver to minimize the value in the cell R28 by changing I28 to K28, by having I28<0 as a constraint.
6. Runs the Solver to minimize the value in the cell M30 by changing K30.
7. Runs the Solver to minimize the value in the cell G54 by changing E54.
8. Runs the Solver to minimize the value in the cell G55 by changing E55.
9. Selects and copies the values in the values in cells B25 to B68 of the Calculation worksheet.
10. Transposes and pastes the values in the row 1 of the Results worksheet.
11. Insert a new row on row 1 to shift the row with existing values down and avoid overwriting.
12. Selects the Data worksheet and deletes the row 3 to shift up the next row of data.
13. Replicates steps 1 to 12 until there is no data in cell A3 of Data worksheet.

14. Copies the title of the data available in cells A25 to A68 of the Calculation worksheet to row 1 of the Results worksheet.

5.5. Limitations of the Methodology

The proposed methodology and Excel macro can also be used to identify the pavement structures with better resilience to the flooding by grouping sections based on the flooding duration (no flooding, single and multiple day flooding) and on design features such as pavement type, functional class, age or time from the most recent resurfacing or reconstruction, subgrade soil type, traffic volume, layer thickness. In the case of networks with large number of sections, grouping done based on multiple criteria can allow detailed comparison and identification of design feature with more impact on the resiliency to flooding. ANOVA and MANOVA technique can be used to compare the standard deviate, Z-score, calculated for the drop in pavement condition index (PCI) for sections in different groups, as shown in Subsection 5.2.9.

The methodology proposed is more effective if data from multiple condition surveys done before the flooding is available since the methodology relies on the accuracy of PCI and IRI prediction models. These models are more accurate is conditions data from more surveys done over the years are available for each section. In this way, the PSI and IRI models are built based on multiple observations.

Chapter 5 presented a process for identifying the sections of street or roads in a network that have been flooded and the duration of flooding using GIS data. The example show is for the GIS data collected during Hurricane Harvey for the City of Houston. However, at the time this report was written (August 2019), the City of Houston could not provide sufficient data to use the methodology. Data only for one condition survey before Hurricane Harvey and one survey after was available for local streets. Therefore, models for PCI and IRI could not be developed for local streets. Condition survey data was available for three surveys done before Hurricane Harvey but the first survey after Hurricane Harvey on principal arterials / collectors was not finalized. Therefore, the methodology could not be used for principal arterial / collector streets either.

The Texas Department of Transportation considers PMS data as sensitive information. Therefore, no PMS data was provided to run the methodology for the state highways in the area affected by Hurricane Harvey.

6. CONCLUSIONS

In order to estimate the damage caused by flooding, such that caused by Hurricane Harvey, on a road or street network a new methodology has been developed. The methodology consists of two parts:

a. The identification of flooded street or pavement sections using GIS flood maps that can be overlapped with street GIS maps normally used for pavement management systems (PMS) by cities or state authorities.

b. The estimation of the increase in rehabilitation works due to the damage caused by flooding directly or indirectly. An example Excel macro was created to illustrate the estimation process. The methodology estimates the increase in rehabilitation costs due to the fact that many rehabilitation works must be done earlier than anticipated before the flooding. The methodology also estimated the increase in fuel consumption caused by the increased in pavement roughness if the rehabilitation works are done when anticipated before the flooding.

The methodology and the Excel macro can also be used to identify the pavement structures with better resilience to the flooding by grouping sections based on the flooding duration (no flooding, single and multiple day flooding) and on design features such as pavement type, functional class, age or time from the most recent resurfacing or reconstruction, subgrade soil type, traffic volume, layer thickness. In the case of networks with large number of sections, grouping done based on multiple criteria can allow detailed comparison and identification of design feature with more impact on the resiliency to flooding. ANOVA and MANOVA technique can be used to compare the Z-score values calculated for sections in different groups, as shown in Subsection 5.2.9.

The methodology compares for each street or pavements section the measured condition after the flooding with that predicted based on data collected in multiple condition surveys before the flooding. Therefore, it considers each road or street section as having unique design features and performance. Other methodologies assume that pavements having some similar design features should have the same performance. This approach is misleading since pavements with identical design features may perform differently due to difference in drainage quality, in geometrical features and in the quality of their construction or rehabilitation.

6.1. Recommendations

The methodology developed estimates the damage caused by flooding, such that caused by Hurricane Harvey, on a road or street network. The methodology should be further refined by:

- Conducting further research to find the optimum evolution curves for both PCI and IRI. In the example Excel macro provided, second order polynomial functions were used. More accurate prediction models may be developed for specific road or street networks based on historical performance data or expert engineering judgment.
- Coupling the methodology with more advanced optimization techniques to study various scenarios in which the rehabilitation of some sections is postponed for the following years. This would allow the programming of rehabilitation works under specific financial constraints. A limitation of the developed methodology is that estimates the increased

rehabilitation costs if all pavements are rehabilitated when their condition reaches critical levels, or trigger values. Therefore, it does not consider that the road or street agency might have limited funding for rehabilitation works.

REFERENCES

1. NOAA. National Centers for Environmental Information (NCEI) U.S. Billion Dollar Weather and Climate Disasters (2019). https://www.ncdc.noaa.gov/.

2. Federal Emergency Management Administration, Significant Flood Events (2019). https://www.fema.gov/significant-flood.

3. Kopp, R. E., Horton R., Little, C. J., Mitrovica, M., Oppenheimer, D. J. Rasmussen, Strauss, B., & Tebaldi, C. (2014). Probabilistic 21st and 22nd century sea-level projections at a global network of tide-gauge sites. *Earth's future*, 2(8), 383-406.

4. Buchanan, M. K., Oppenheimer, M., and Kopp, R. E. (2017). Amplification of flood frequencies with local sea level rise and emerging flood regimes. *Environmental Research Letters*, 12(6), 064009.

5. Chen, X., & Zhang, Z. (2014). Effects of Hurricanes Katrina and Rita flooding on Louisiana pavement performance. In *Pavement materials, structures, and performance* (pp. 212-221).

6. Gaspard, K., Martinez, M., Zhang, Z., & Wu, Z. (2007). Impact of Hurricane Katrina on roadways in the New Orleans Area: technical assistance report (No. 07-2TA). *Louisiana Transportation Research Center*.

7. Helali, K., Robson, M., Nicholson, R., & Bekheet, W. (2008). Importance of a pavement management system in assessing pavement damage from natural disasters: a case study to assess the damage from Hurricanes Katrina and Rita in Jefferson Parish, Louisiana. In *7th International Conference on Managing Pavement Assets*.

8. Vennapusa, P., White, D. J., & Miller, D. K. (2013). Western Iowa Missouri River Flooding--Geo-Infrastructure Damage Assessment, Repair and Mitigation Strategies. *Center for Earthworks Engineering Research*, Iowa State University, IHRB TR-638, 2013.

9. Sultana, M., Chai, G., Martin, Tim, and Chowdhury, S. (2015). "A Study on the Flood Affected Flexible Pavements in Australia." In *Proceedings of the 9th International Conference on Road and Airfield Pavement Technology*.

10. Sultana, M., Chai, G., Martin, T., & Chowdhury, S. (2016). Modeling the postflood short-term behavior of flexible pavements. *Journal of Transportation Engineering*, 142(10), 04016042.

11. Sultana, M., Chai, G., Chowdhury, S., Martin, T., Anissimov, Y., & Rahman, A. (2018). Rutting and Roughness of Flood-Affected Pavements: Literature Review and Deterioration Models. *Journal of Infrastructure Systems*, 24(2), 04018006.

12. Mallick, R. B., Radzicki, M. J., Daniel, J. S., & Jacobs, J. M. (2014). Use of system dynamics to understand long-term impact of climate change on pavement performance and maintenance cost. *Transportation Research Record*, 2455(1), 1-9.

13. Mallick, R. B., Tao, M., Daniel, J. S., Jacobs, J., & Veeraragavan, A. (2017). Development of a methodology and a tool for the assessment of vulnerability of roadways to flood-induced damage. *Journal of Flood Risk Management*, 10(3), 301-313.

14. Shamsabadi, S. S., Tari, Y. S. H., Birken, R., & Wang, M. (2014, July). Deterioration forecasting in flexible pavements due to floods and snow storms. In *the Proceedings of the 7th European Workshop on Structural Health Monitoring.*

15. Khan, M. U., Mesbah, M., Ferreira, L., & Williams, D. J. (2017). Estimating pavement's flood resilience. *Journal of Transportation Engineering*, Part B: Pavements, 143(3), 04017009.

16. Elshaer, M.H. (2017). Assessing the mechanical response of pavements during and after flooding. *Doctoral dissertation*, University of New Hampshire.

17. Asadi, M., Kottayi, N. M., Tirado, C., Mallick, R. B., Mirchi, A., & Nazarian, S. (2019). Framework for Rigorous Analysis of Moisture-Related Structural Damage in Flexible Pavements. *Transportation Research Record*, 0361198119852606.

18. NOAA National Water Center, E. Boghici, D. Arctur (2018). NOAA NWC - Harvey NWM-HAND Flood Extents, *HydroShare*, https://doi.org/10.4211/hs.fe85a680d0144.

19. Chatti, K., & Zaabar, I. (2012). Estimating the effects of pavement condition on vehicle operating costs (Vol. 720). *Transportation Research Board*.

20. Greenhouse Gas Emissions from a Typical Passenger Vehicle. 2018. Publication EPA420-F-18-008. U.S. Environmental Protection Agency.

APPENDIX A

```
Sub Comp()
'
' Comp Macro
'
' Keyboard Shortcut: Ctrl+m
'
i = 1
Do While Cells(3, 1) <> ""
    Sheets("Data").Select
    Range("A3:T3").Select
    Selection.Copy
    Sheets("Calculation").Select
    Range("B25").Select
    Selection.PasteSpecial Paste:=xlPasteValues, Operation:=xlNone, SkipBlanks _
      :=False, Transpose:=True
    SolverOk SetCell:="$R$23", MaxMinVal:=2, ValueOf:=0, ByChange:="$I$23:$K$23", _
      Engine:=1, EngineDesc:="GRG Nonlinear"
    SolverAdd CellRef:="$I$23", Relation:=3, FormulaText:="0"
    SolverSolve True
    SolverOk SetCell:="$M$25", MaxMinVal:=2, ValueOf:=0, ByChange:="$K$25", _
      Engine:=1, EngineDesc:="GRG Nonlinear"
     SolverSolve True
    SolverOk SetCell:="$R$28", MaxMinVal:=2, ValueOf:=0, ByChange:="$I$28:$K$28", _
      Engine:=1, EngineDesc:="GRG Nonlinear"
    SolverAdd CellRef:="$I$28", Relation:=1, FormulaText:="0"
    SolverSolve True
    SolverOk SetCell:="$M$30", MaxMinVal:=2, ValueOf:=0, ByChange:="$K$30", _
      Engine:=1, EngineDesc:="GRG Nonlinear"
    SolverSolve True
    SolverOk SetCell:="$G$54", MaxMinVal:=2, ValueOf:=0, ByChange:="$E$54", _
      Engine:=1, EngineDesc:="GRG Nonlinear"
    SolverSolve True
    SolverOk SetCell:="$G$55", MaxMinVal:=2, ValueOf:=0, ByChange:="$E$55", _
      Engine:=1, EngineDesc:="GRG Nonlinear"
    SolverSolve True
    Range("B25:B68").Select
    Selection.Copy
    Sheets("Results").Select
    Range("A1").Select
    Selection.PasteSpecial Paste:=xlPasteValues, Operation:=xlNone, SkipBlanks _
      :=False, Transpose:=True
    Rows("1:1").Select
    Application.CutCopyMode = False
    Selection.Insert Shift:=xlDown, CopyOrigin:=xlFormatFromLeftOrAbove
    Sheets("Data").Select
```

```
    Rows("3:3").Select
    Selection.Delete Shift:=xlUp

  i = i + 1
  Loop
  Sheets("Calculation").Select
  Range("A25:A68").Select
  Selection.Copy
  Sheets("Results").Select
  Range("A1").Select
  Selection.PasteSpecial Paste:=xlPasteValues, Operation:=xlNone, SkipBlanks _
      :=False, Transpose:=True
End Sub
```